

Photochemistry

How to cite:

International Edition: doi.org/10.1002/anie.202010710

German Edition: doi.org/10.1002/ange.202010710

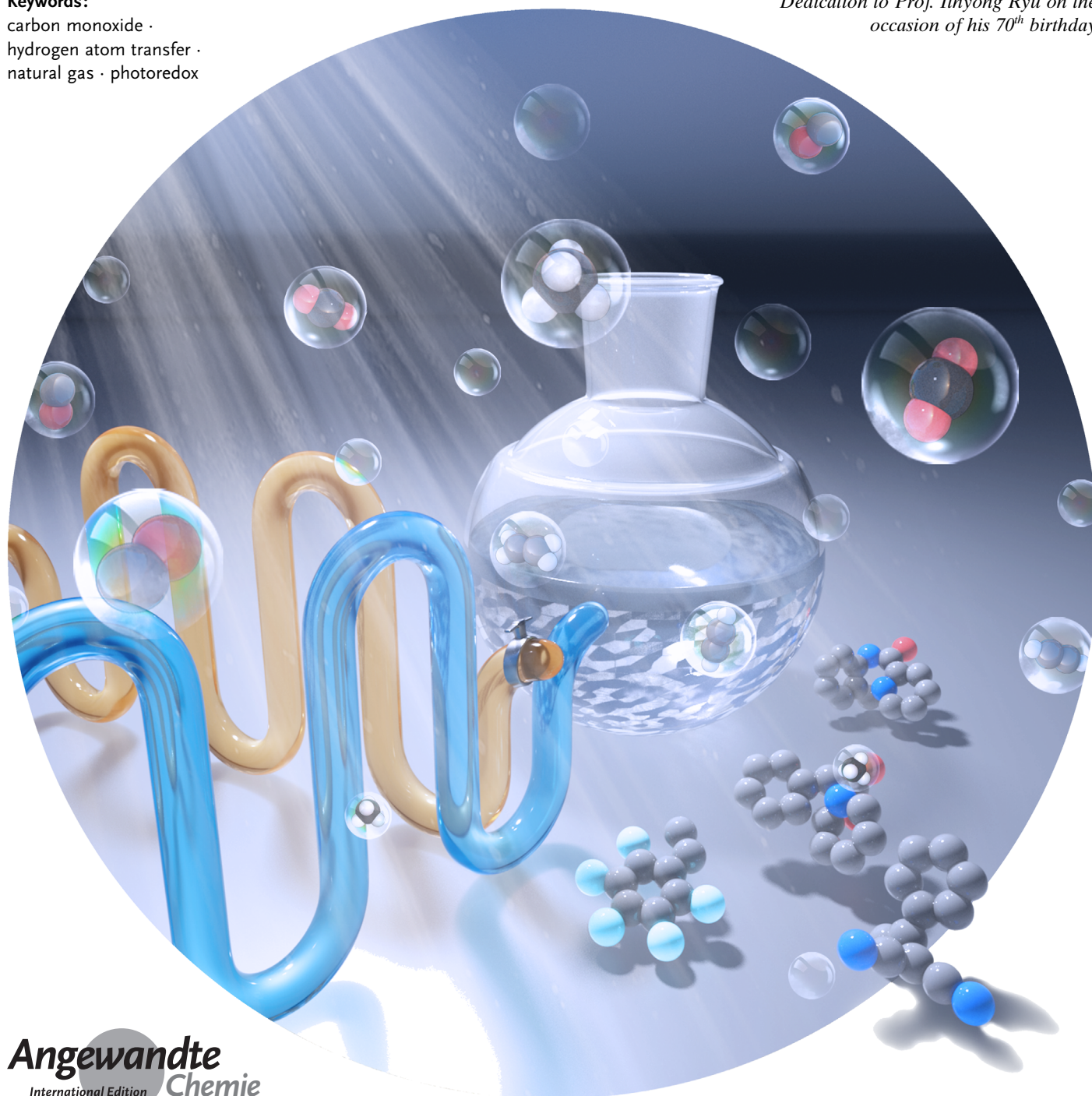
# Light-Promoted Organic Transformations Utilizing Carbon-Based Gas Molecules as Feedstocks

Bin Cai<sup>+</sup>, Han Wen Cheo<sup>+</sup>, Tao Liu, and Jie Wu\*

**Keywords:**

carbon monoxide ·  
hydrogen atom transfer ·  
natural gas · photoredox

*Dedication to Prof. Ilhyong Ryu on the  
occasion of his 70<sup>th</sup> birthday*



Angewandte  
International Edition  
Chemie

Wiley Online Library

© 2020 Wiley-VCH GmbH

Angew. Chem. Int. Ed. 2021, 60, 2–33

These are not the final page numbers!

**C**arbon-based gas molecules are readily available feedstocks and are widely used in industry as building blocks or fuels. However, their application in the synthesis of fine chemicals has been hampered due to operational complexity, poor reaction efficiency and selectivity. Recent development of photoredox-promoted transformations using such gaseous reagents has received considerable attention from the synthetic community. In this review, efforts in developing light-promoted organic transformations using carbon-based natural gases as C1 or C2 feedstocks and to overcome the associated challenges are briefly summarized.

## 1. Introduction

Carbon-based gas molecules are abundant and readily available feedstocks for use in chemical synthesis. Carbon monoxide (CO) and carbon dioxide (CO<sub>2</sub>) are substantially produced from the combustion of carbon-based substrates, and ethylene, acetylene, ethane and methane are among the most common carbon-based natural gases employed in chemical industry as C1 or C2 building blocks for chemical synthesis. For example, carbon dioxide has been widely used in the synthesis of polycarbonates and cyclic carbonates and for the production of urea through the Bosch-Meiser process.<sup>[1]</sup> Due to the ease of access to these gases, synthetic strategies have been developed to synthesize value-added fine chemicals from these simple and abundant feedstock compounds.<sup>[2]</sup> In this context, the development of light-promoted transformations utilizing carbon-based natural gases has gained momentum and is briefly summarized in this review.

## 2. Carbon Monoxide

Carbon monoxide is an inexpensive and abundant single-carbon source that is used in various carbonylation reactions. Early 20th century studies of the Fisher Tropsch synthesis and hydroformylation reactions have led to a better understanding of carbonylation reactions.<sup>[3]</sup> These reactions are now widely used in industries to produce valuable fine chemicals. For instance, the industrial production of acetic acid is through the carbonylation of methanol employing the Monsanto or Cativa process.<sup>[4]</sup> However, precautions are necessary due to the high toxicity of CO when used as the starting material.

Carbonylation using CO as the carbonyl source provides an efficient and atom-economic way to install a variety of carbonyl-based functional groups. A useful method is the radical carbonylation. However, this method did not receive attention until the early 1990s, when the groups of Bakac, Goldman and Ryu independently reported kinetic studies of radical carbonylation.<sup>[5]</sup> Since then, a series of radical-based carbonylation transformations, including light-mediated radical carbonylation reactions, have been developed.

## From the Contents

1. Introduction	3
2. Carbon Monoxide	3
3. Carbon Dioxide	9
4. Gaseous Alkenes and Alkynes	25
5. Gaseous Alkanes	26
7. Summary and Outlook	29

### 2.1. Light-Promoted Radical Carbonylation in the Absence of Photosensitizers


In 1939, Faltings reported that acetone was produced when ethane and CO were irradiated with UV light.<sup>[6]</sup> Following Faltings' discovery, Ryu et al. demonstrated a light-promoted, atom-transfer-carbonylative three-component coupling reaction between  $\alpha$ -phenylselenides, terminal alkenes, and CO to afford a variety of adducts (Scheme 1).<sup>[7]</sup> A proposed mechanism involved the selenide **1** undergoing light-promoted homolysis to generate radical species **3**. Subsequent radical addition of **3** to an olefin **2** produces an alkyl radical **4**, which undergoes a second radical addition with CO to yield an acyl radical **5**. A group transfer of the phenylselenenyl group leads to the formation of the acyl selenide **6**. Various products (**6a–6f**) could be synthesized in this manner. Notably, a sophisticated reactor system is required in light-promoted carbonylation with high pressure CO (Figure 1). The reaction was conducted in a stainless steel autoclave with quartz glass windows, which enables chemical transformations with high pressure gaseous reagents under light-irradiation.

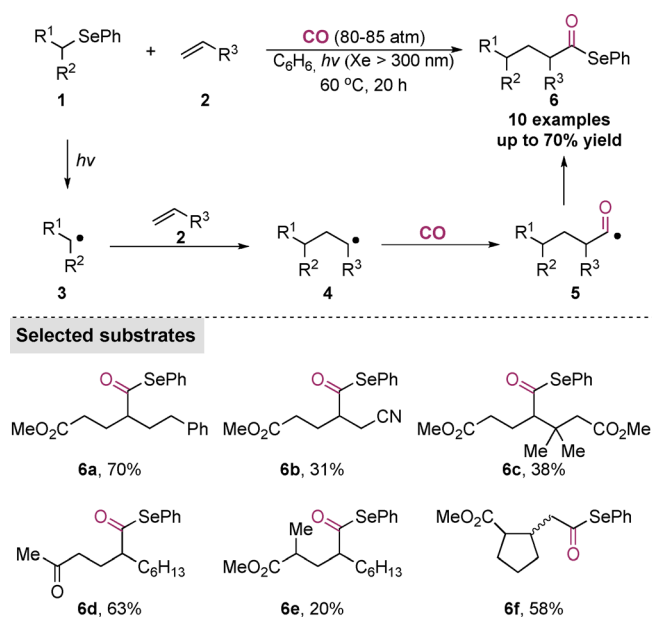
Based on the fact that the C–I bond in an alkyl iodide could be homolytically cleaved to generate an alkyl radical under light irradiation,<sup>[8]</sup> the Ryu group reported a light-mediated catalyst-free esterification of alkyl iodides with alcohols (Scheme 2A).<sup>[9]</sup> The endothermic transfer of iodine from the alkyl iodide to an acyl radical was aided by the addition of a base. Moreover, the same protocol could be

[\*] H. W. Cheo,<sup>[†]</sup> T. Liu, Dr. J. Wu  
Department of Chemistry, National University of Singapore  
3 Science Drive 3, Singapore 117543 (Republic of Singapore)  
E-mail: chmjie@nus.edu.sg

Dr. B. Cai<sup>[†]</sup>  
Department of Chemistry, Scripps Research  
10550 North Torrey Pines Road, La Jolla, California 92037 (USA)  
Dr. J. Wu  
National University of Singapore (Suzhou) Research Institute  
377 Lin Quan Street, Suzhou Industrial Park, Suzhou, Jiangsu 215123  
(P. R. China)

[†] These authors contributed equally to this work.

 The ORCID identification number(s) for the author(s) of this article can be found under <https://doi.org/10.1002/anie.202010710>.



**Scheme 1.** Photo-induced phenylselenenyl group transfer carbonylation.

employed for the amidation of alkyl iodides using amines as the nucleophiles (Scheme 2B).<sup>[10]</sup> Syntheses of <sup>11</sup>C radiolabeled alkyl acids and related derivatives have also been achieved utilizing this protocol.<sup>[11]</sup> The same group extended this strategy to carbonylation of aryl iodides irradiated by a 500 W xenon (Xe) lamp.<sup>[12]</sup>

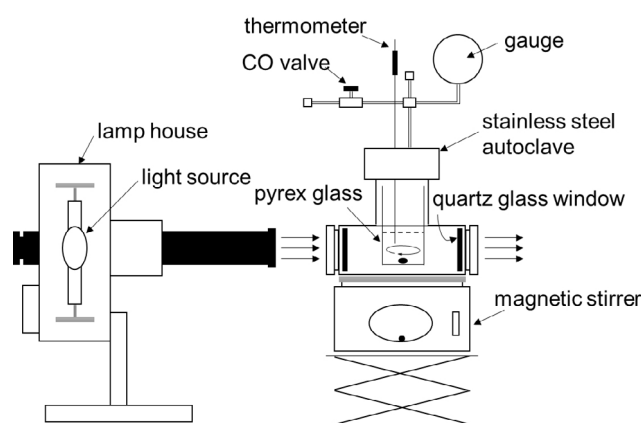
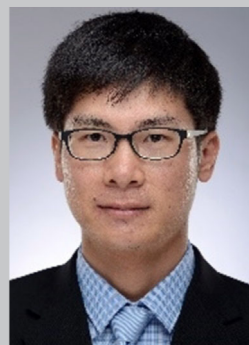


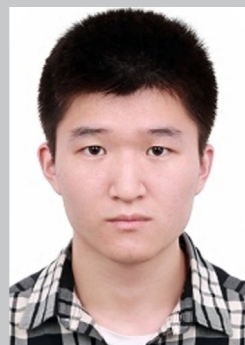
**Figure 1.** Reaction set-up of photocatalyzed carbonylation in the presence of high pressure CO (picture reproduced from ref. [7]).

## 2.2. Light-Promoted C–H Carbonylation through Hydrogen Atom Transfer

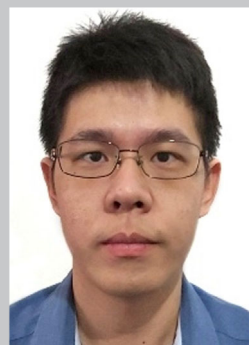
An early discovery of C–H carbonylation was made in 1991 by Crabtree et al., who observed the formation of aldehydes from alkyl radicals generated by mercury photosensitization in the presence of CO.<sup>[13]</sup> Subsequently, the Goldman group demonstrated the synthesis of aldehydes by carbonylation of cyclohexane, catalyzed by aryl ketones under UV light.<sup>[5b]</sup> Mechanistically, the aromatic ketone catalyst is photo-excited to generate an excited ketone species **16**. A hydrogen atom transfer (HAT) process between cyclohexane and **16** forms a ketyl radical **17** and cyclohexyl radical **18**, which then traps CO to form an acyl radical **19**. A reverse HAT process between **19** and **17** produces the aldehyde product and regenerates the aromatic ketone



Bin Cai was born in Suzhou, China. He received his Ph.D. in organic chemistry at Boston University in August 2018 under the guidance of Prof. James S. Panek. He is now a Postdoctoral Associate with Prof. Dale L. Boger at the Scripps Research, CA, USA.



Tao Liu was born in Jiangxi Province, China. He obtained his B.Sc. in Chemistry under the supervision of Dr. Jin Xie at Nanjing University in June 2020. Currently, he is pursuing his Ph.D. in Dr. Wu's group, and focuses on methodology development under visible-light irradiation by taking use of continuous micro-flow reactors.

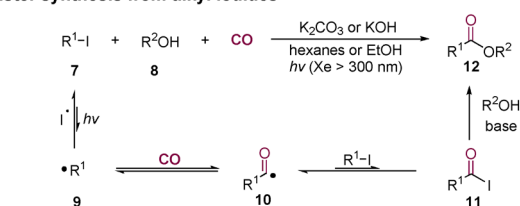


Han Wen Cheo was born and raised in Singapore. He obtained his B.Sc. in Chemistry at the National University of Singapore and M.Sc. in Chemistry in Dr. Wu's group.

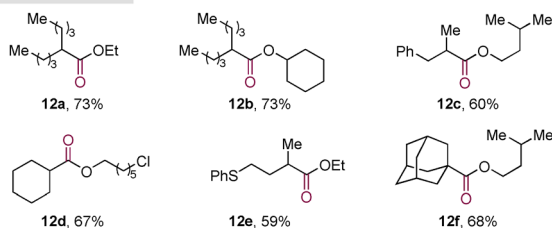


Jie Wu was born and raised in Sichuan Province, China. He received his Ph.D. in organic chemistry at Boston University in 2012, under the supervision of Prof. James S. Panek. He was then appointed as a Skol-Tech Postdoctoral Fellow with Prof. Timothy F. Jamison and Prof. T. Alan Hatton at MIT. After working as a senior scientist in Snapdragon Chemistry Inc., he joined the chemistry department of NUS in July 2015 as an Assistant Professor. His research group focuses on photo organic synthesis, continuous-flow synthesis, and automated synthesis.

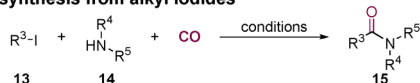
## A) Ester synthesis from alkyl iodides



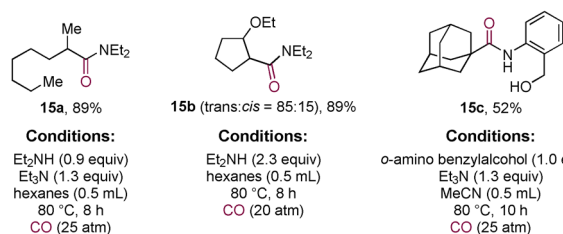
## Selected substrates



## B) Amide synthesis from alkyl iodides

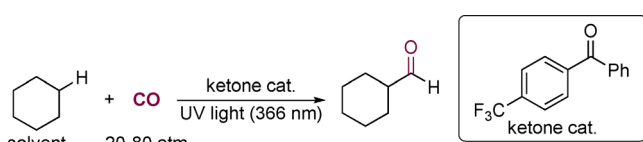


## Selected substrates

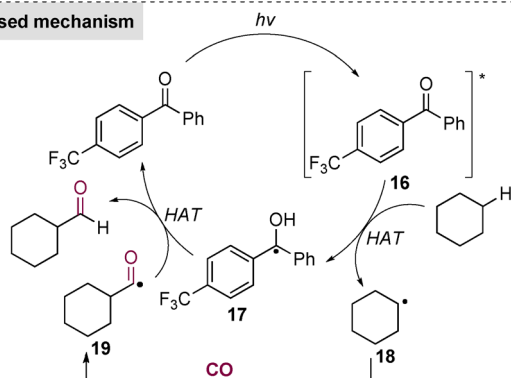


Scheme 2. Photo-induced carbonylation of alkyl iodides.

catalyst (Scheme 3). In 1995, the Hill group reported a tetrabutylammonium decatungstate (TBADT)-catalyzed alkane carbonylation under 1 atm CO, irradiated with a 550 W Hg lamp (> 280 nm). A TON of 54 was achieved for this reaction using cyclohexane as the substrate.<sup>[14]</sup> Ryu and co-workers

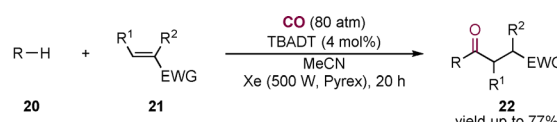


## Proposed mechanism

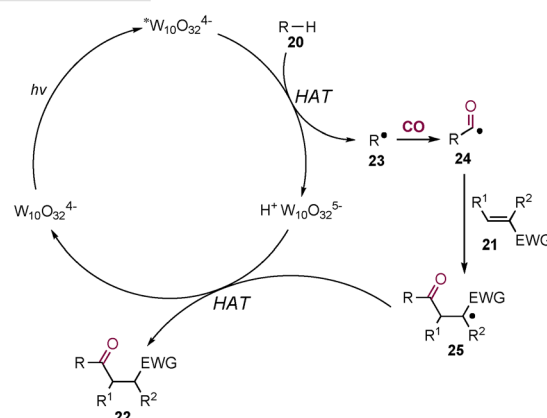


Scheme 3. Aryl ketone catalyzed carboxylation of cyclohexane under UV light.

realized a three-component coupling reaction involving alkanes, CO at high pressure (80 atm), and electron deficient alkenes, employing TBADT as a catalyst and a xenon (Xe) lamp light source.<sup>[15]</sup> They envisioned that TBADT would be photo-excited to generate an excited polyoxotungstate anion  $^*[W_{10}O_{32}]^{4-}$ , which promotes the formation of a carbon-centered radical **23** through an HAT process with an alkane (Scheme 4). Subsequent radical addition to CO delivers an acyl radical **24**, which is trapped by an electron-deficient alkene to selectively form a radical adduct **25**. A second HAT process could transfer the hydrogen atom from the reduced tungstate anion to the radical adduct **25** to form the desired product **22** and regenerate the TBADT catalyst. In addition, Ryu et al. showed that  $\beta$ -carbon carbonylation of cyclopentanones and aliphatic nitriles could be achieved with a similar protocol to yield  $\beta$ -alkylated ketones.<sup>[16]</sup> Alternatively, acyl hydrazide compounds could be obtained by trapping the acyl radical using diisopropyl azodicarboxylate.<sup>[17]</sup>



## Proposed mechanism

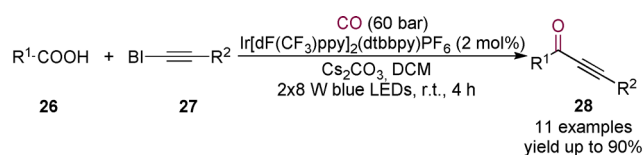


Scheme 4. TBADT-catalyzed three-component carbonylation using alkanes.

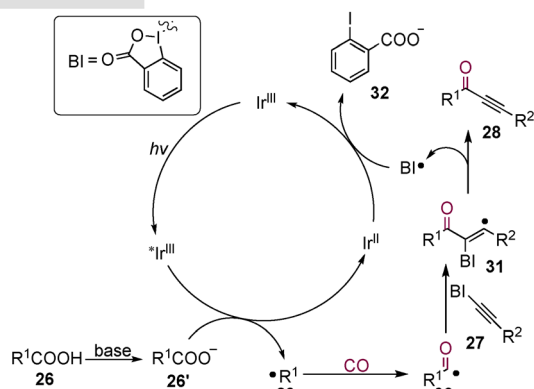
## 2.3. Recent Development in Photoredox-Promoted Carbonylation

The widely utilized iridium (Ir)- and ruthenium (Ru)-based photosensitizers have showed excellent catalytic activity in carbonylation reactions. In 2015, the Xiao group developed a visible-light-promoted decarboxylative carbonylative alkylation reaction between aliphatic carboxylic acids and benzodioxolone-substituted alkynes catalyzed by Ir[dF(CF<sub>3</sub>)ppy]<sub>2</sub>(dtbbpy)PF<sub>6</sub>, generating ynones in good to excellent yields (Scheme 5).<sup>[18]</sup> It was proposed that the reaction is initiated by a single-electron oxidation of the carboxylic anion **26'** by the excited state of the iridium(III) photocatalyst to generate an alkyl radical **29**. Subsequent radical addition of **29** to CO gives the acyl radical **30**, which undergoes a second radical addition to the alkyne **27** to yield





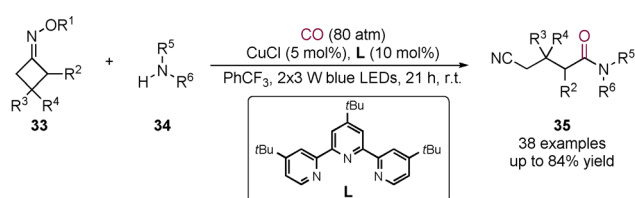
## Proposed mechanism



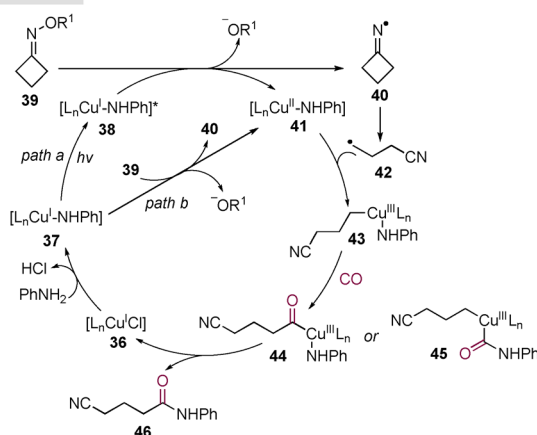
Scheme 5. Ir-catalyzed decarboxylative carbonylative alkylation.

a vinyl radical **31**. An elimination of a benzodioxolone (BI) radical produces the desired ynone **28**. In 2018, Bousquet et al. developed a carboxylation reaction of aryldiazonium salts employing  $\text{H}_2\text{O}$  as a nucleophile and  $\text{Ru}(\text{bpy})_3\text{Cl}_2$  as the photocatalyst.<sup>[19]</sup> The Polyzos group reported a visible-light-mediated  $\text{Ir}(\text{ppy})_2(\text{dtbbpy})\text{PF}_6$ -catalyzed annulative alkoxy-carbonylation of alkenyl-tethered aryldiazonium salts to yield 2,3-dihydrobenzofurans products in a continuous flow system.<sup>[20]</sup> In 2019, the Xiao group reported an efficient copper-catalyzed radical aminocarbonylation of cycloketone oxime esters in the presence of CO and amines under visible-light irradiation.<sup>[21]</sup> Mechanistically, the authors proposed a visible light-driven  $\text{Cu}^{\text{I}}/\text{Cu}^{\text{II}}/\text{Cu}^{\text{III}}$ -based catalytic cycle (Scheme 6). The in situ generated copper(I) complex **36** reacts with phenylamine to form a new copper(I) complex **37**, which after light irradiation forms the photoexcited copper complex **38**. A subsequent SET-mediated reduction of **39** by **38** affords an iminyl radical **40** and copper(II) complex **41** (path a). Alternatively, **40** and **41** could be generated by reduction of **39** by **37** (path b). The iminyl radical **40** would then undergo a selective  $\beta\text{-C-C}$  bond scission to give a cyanoalkyl radical **42**, which couples with **41** to form a high-valent  $\text{Cu}^{\text{III}}$  complex **43**. Subsequent coordination and insertion of CO to **43** would lead to the formation of acylcopper intermediate **44** or **45**. Reductive elimination of the acylcopper complex produces cyanoalkylated amide **46** and regenerates the  $\text{Cu}^{\text{I}}$  **36**.

Organic dyes have been widely used as photoredox catalysts to replace the costly Ir and Ru noble metals, and have exhibited excellent photo-catalytic activities.<sup>[22]</sup> In this context, the Xiao group reported a visible-light-promoted alkoxy-carbonylation reaction of aryldiazonium salts under 80 atm of CO, using fluorescein as the photocatalyst (Scheme 7A).<sup>[23]</sup> A wide range of substituted aryldiazonium salts and alcohols are well tolerated in this reaction. The photocatalytic carboxylation protocol can be used with chiral alcohols to obtain enantiomerically pure products (**49e**, **49f**).

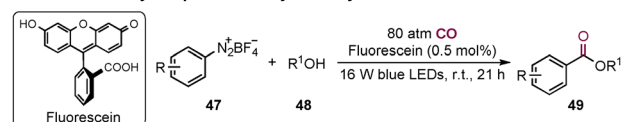


## Proposed mechanism

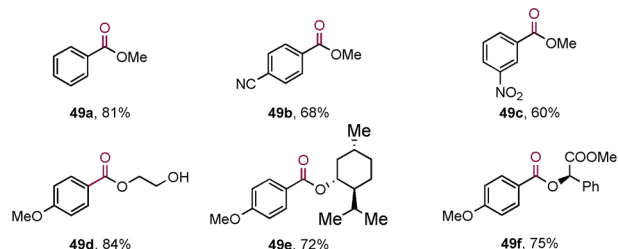


Scheme 6. Photoinduced copper-catalyzed radical aminocarbonylation of cycloketone oxime esters.

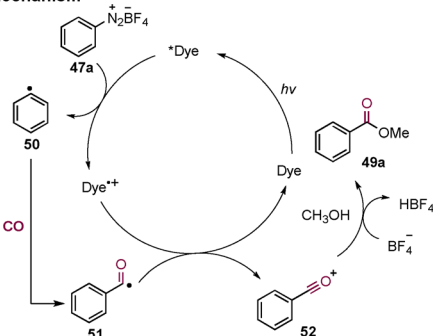
## A) Fluorescein-catalyzed photo alkoxy-carbonylation



## Selected substrates



## B) Proposed mechanism



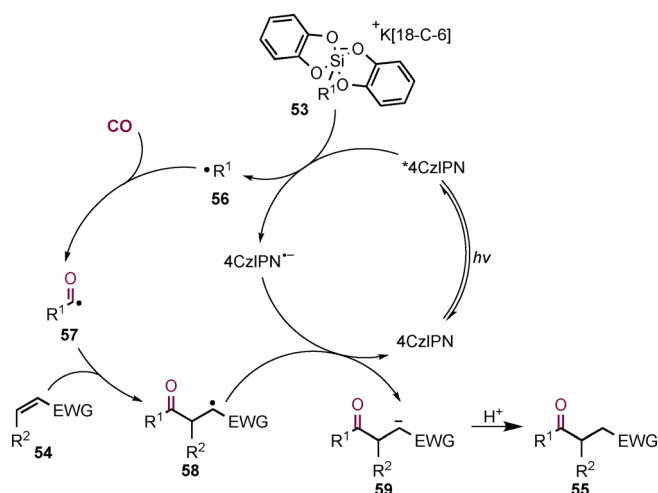
Scheme 7. Fluorescein-catalyzed photo alkoxy-carbonylation.

Based on control experiments, a plausible mechanism for this reaction was proposed as shown in Scheme 7B. The catalytic cycle begins with a single electron reduction of aryldiazonium salt by the light-excited photocatalyst to

generate a phenyl radical **50** and a fluorescein radical cation. The phenyl radical **50** subsequently reacts with CO to yield an acyl radical **51**, which is oxidized by the fluorescein radical cation to give benzylideneoxonium ion **52**. Finally, a nucleophilic attack by an alcohol to the benzylideneoxonium ion **52** yields the desired ester product **49a**.

In 2015, Wangelin and co-workers demonstrated that the same transformation could also proceed employing eosin Y sodium salts under green light irradiation.<sup>[24]</sup> Later, Gu and co-workers reported an eosin Y-catalyzed aryl ketone and indol-3-yl aryl ketone synthesis using aryldiazonium salts and heteroarenes.<sup>[25]</sup>

In 2019, Fensterbank and co-workers demonstrated a three-component carbonylation reaction between organosilicates, CO and alkenes (Scheme 8).<sup>[26]</sup> A wide range of alkyl silicates and electron-withdrawing substituents on the alkenes are tolerated in the reaction, yielding products in moderate to good yields. Interestingly, a non-carbonylated product **55t** was obtained when the reaction was conducted using disulfonylethene. The strong radical accepting character of the sulfonyl group appeared to lead to the direct addition of the cyclohexyl radical to the Michael acceptor without carbonylation. It was also demonstrated that when allylsulfones were employed,  $\beta,\gamma$ -unsaturated ketone products were obtained through the elimination of a phenyl sulfinate radical.<sup>[26a]</sup> Recently, the same group expanded this method to the synthesis of amides in the presence of amines and  $\text{CCl}_4$  (as a halogen donor).<sup>[27]</sup> The reaction was thought to be initiated through photo excitation of the photocatalyst, 1,2,3,5-tetrakis(carbazol-9-yl)-4,6-dicyanobenzene (4CzIPN)

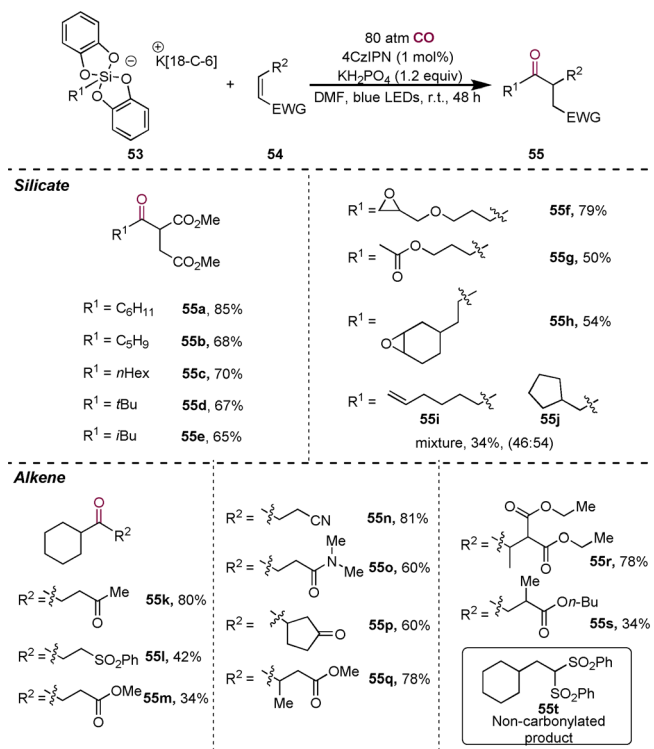


Scheme 9. Proposed mechanism for unsymmetrical ketone synthesis.

to the excited state  $4\text{CzIPN}^*$ , which can oxidize the silicate to yield an alkyl radical **56** and silicon cation along with a reduced  $4\text{CzIPN}^-$  (Scheme 9). The resulting alkyl radical **56** is then trapped by CO to form an acyl radical **57**, which can undergo a second radical addition to the alkene to generate the radical adduct **58**. The adduct **58** is then reduced by  $4\text{CzIPN}^-$  to yield a carbanion **59**, which is protonated to form the desired product **55**. In the allyl sulfonate reaction, the eliminated phenyl sulfinate radical is reduced to regenerate the photocatalyst.

#### 2.4. Light-Promoted Transition Metal-Catalyzed Carbonylation

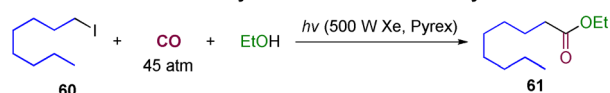
In the 1980s, the groups of Watanabe and Suzuki independently observed that the reaction efficiency of transition metal-catalyzed carbonylation of alkyl iodides could be improved under light irradiation.<sup>[28]</sup> They proposed that CO would insert into the alkyl-metal species to yield an acyl-metal species. This was further extensively evaluated by Ryu et al., who discovered that Pd complexes could accelerate the photo-induced atom-transfer-carbonylation (ATC) reaction of a wide range of alkyl iodides.<sup>[29]</sup> For example, the addition of Pd complexes led to improved yields (from 54 % to 87 %) and shortened reaction time (from 50 h to 14 or 16 h) in the ATC reaction between 1-iodooctane, CO, and ethanol (Scheme 10A).<sup>[30]</sup> They proposed that the radical initiation step may involve a single electron transfer (SET) process from  $\text{Pd}^0$  to cleave the C–I bond in an alkyl iodide **60**, generating a  $\text{Pd}^{\text{I}}$  species and an alkyl radical **62**. The resulting radical **62** could then undergo a radical addition to carbon monoxide to form an acyl radical **63**, which can couple with  $\text{Pd}^{\text{I}}\text{-I}$  to give a  $\text{Pd}^{\text{II}}$  complex **64**. Subsequent metathesis of **64** with ethanol and reductive elimination produced an ethyl ester **61** (Scheme 10B). Importantly, terminal alkynes, boronic acids, amine and alkenes were also found to be able to participate in the three-component reactions to form the corresponding carbonyl products.<sup>[31]</sup> In addition, this strategy was applied to the synthesis of the (–)-hinokinin precursor and dihydrocapsaicin.<sup>[32]</sup> Interestingly, cyclized double car-



Scheme 8. Scope of the three-component reaction between organosilicates, CO, and alkenes.

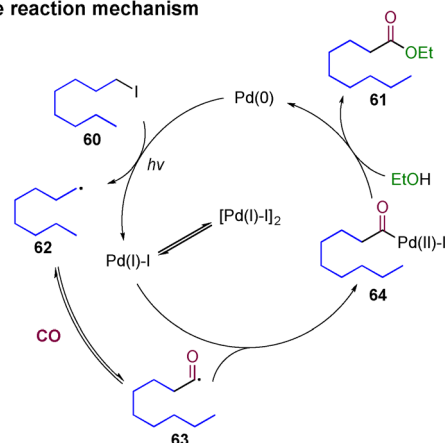


## A) Acceleration of the ATC by the addition of Pd catalysts

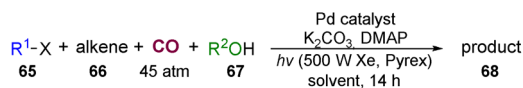


Conditions	Time	Yield
no Pd catalyst	50 h	54%
Pd(PPh <sub>3</sub> ) <sub>4</sub> (5-5.7 mol%)	16 h	87%
Pd <sub>2</sub> (CNMe) <sub>6</sub> (PF <sub>6</sub> ) <sub>2</sub> (2 mol%)	14 h	87%

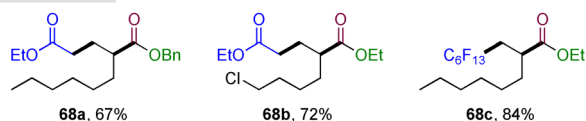
## B) Possible reaction mechanism



## C) Four-component coupling reactions



## Selected substrates

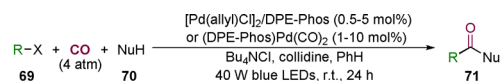


**Scheme 10.** Light-promoted Pd-catalyzed carbonylation and the proposed mechanism.

bonylation products were obtained in good yields when 4-alkenyl iodides were used in the reactions. By light irradiation of a Pd catalyst, the authors also achieved four-component coupling reactions between iodoalkanes, alkenes, alcohols, and CO (Scheme 10C). It is noteworthy that alkyl chloride was tolerated (**68b**) and perfluorohexyl iodide proceeded effectively to furnish ester **68c**.

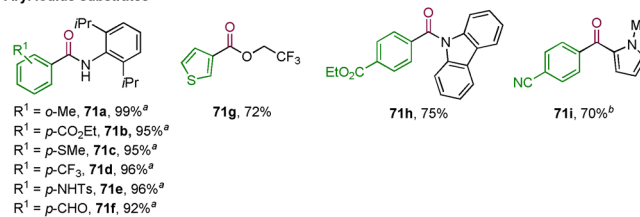
Notwithstanding the efforts devoted to enabling carbonylation with CO, limitations such as the requirement for high pressure CO and harsh conditions, narrow substrate scopes still exist, and prevent the further development and application of these methods. The observation by the Ryu group<sup>[29]</sup> that the efficiency of palladium-promoted carbonylation could be improved by light, inspired Arndtsen et al. to develop highly efficient palladium-catalyzed photo-carbonylation reactions.<sup>[33]</sup> They questioned whether visible light could drive both the oxidative addition and the reductive elimination in one catalytic cycle. Their detailed reaction optimization and mechanistic studies suggested that light-induced single-electron transfer from Pd<sup>0</sup> to aryl iodide, a radical-induced oxidative addition, was followed by formation of acyl radicals and a radical-involved reductive elimination. This breakthrough in the activation mode in

light-induced CO carbonylation allowed carbonylation to proceed under ambient conditions, low pressure of CO, and with challenging aryl or alkyl halides and nucleophiles, generating valuable carbonyl derivatives such as acid chlorides, esters, amides, or ketones (Scheme 11). Both aryl- and alkyl- iodides and bromides are reactive toward carbonylation. Heterocycles (**71g**, **71i**, **71o**, **71r**, **71s**, **71u**), sterically hindered alkyl halide (**71t**) and steroidal halide (**71v**) were all well-tolerated.

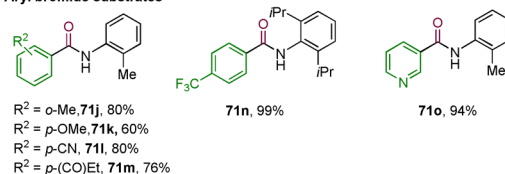


## Selected substrates

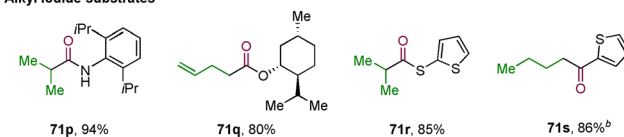
## Aryl iodide substrates



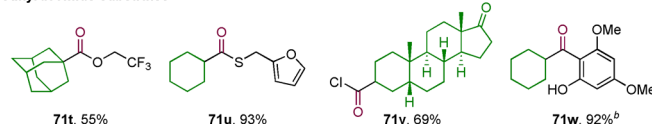
## Aryl bromide substrates



## Alkyl iodide substrates

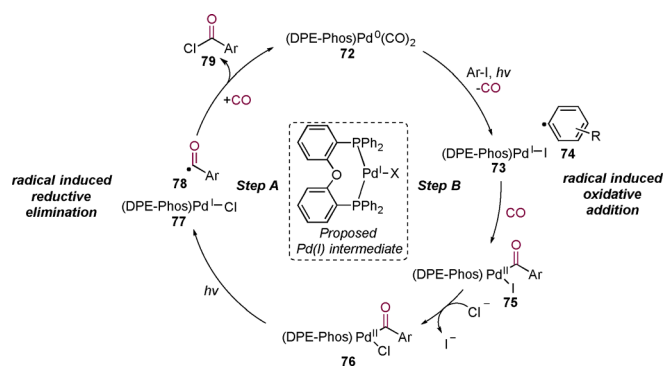


## Alkyl bromide substrates



**Scheme 11.** Selected substrate scope of dual light-driven Pd-catalyzed carbonylation. <sup>a</sup> 14 W light. <sup>b</sup> 1) 40 W blue LED, 5 mol % (DPE-Phos)Pd(CO)<sub>2</sub>, Bu<sub>4</sub>NCl, PhH; 2) DCE, arene (10 equiv), AlCl<sub>3</sub>, r.t.

A plausible, experiment-based mechanism for this reaction was proposed (Scheme 12). Light-induced single-electron transfer from Pd<sup>0</sup> complex **72** to aryl iodide leads to the formation of a Pd<sup>I</sup> complex **73** and an aryl radical **74**. Subsequent oxidative addition of the putative Pd<sup>I</sup> complex **73** with CO and the aryl radical **74** leads to the formation of Pd<sup>III</sup> complex **75**. Notably, this proposed radical-induced oxidative addition pathway with aryl bromides and alkyl iodides is not feasible under thermal conditions, demonstrating the unique role of visible light in this oxidative addition. Subsequent halide exchange produces a Pd complex **76**. Light excitation of **76** would presumably lead to the formation of acyl radical **78**, which after chlorine abstraction from **77** affords an acid chloride **79**. Importantly, the light irradiation reduces the reductive elimination to low energy barriers.



**Scheme 12.** Proposed plausible mechanism for the dual light-driven Pd-catalyzed carbonylation.

In summary, studies on light-promoted radical carbonylation with CO have been briefly summarized. Radicals generated by light-induced bond homolysis, HAT processes, or redox processes can react with CO to form transient acyl radicals with or without the assistance of transition-metals, enabling a straightforward strategy for construction of a wide range of carbonylated compounds. The requirement however for high pressure CO to avoid decarbonylation, in comparison to conventional transition-metal-catalyzed carbonylation, remains a barrier to its broad application. A promising direction to achieve mild and practical carbonylation is to merge light activation with transition-metal catalysis.

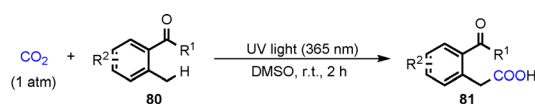
### 3. Carbon Dioxide

Carbon dioxide (CO<sub>2</sub>) is an attractive and renewable C1 feedstock due to its high natural abundance, low cost and lack of toxicity. A number of strategies, such as transition metal-catalyzed and light-mediated carboxylation, have been developed to address its thermodynamic stability and kinetic inertness and convert CO<sub>2</sub> into carboxylic acids and derivatives.<sup>[34]</sup> Compared with conventional methods, the light-mediated systems are more environmentally friendly and can bypass the need for excess metallic reagents or harsh conditions. Pioneering studies in light-driven CO<sub>2</sub> fixation were first seen in the twentieth century, but the reported systems suffered from narrow substrate scopes and poor reaction efficiency and selectivity.<sup>[35]</sup> Major breakthroughs have been made in recent years, especially in the area of photocarboxylation.

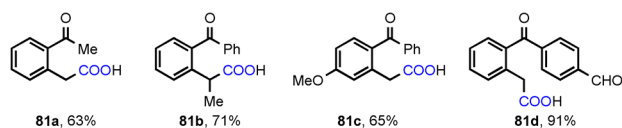
#### 3.1. UV Light-Promoted Carboxylation Using Carbon Dioxide

##### 3.1.1. UV Light-Promoted Carboxylation of C(sp<sup>3</sup>)-H bonds

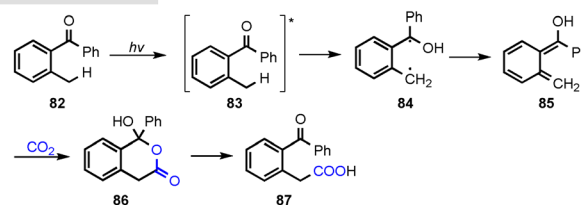
Direct C-H carboxylation through activation of the C-H bond is an atom- and step-economic process for synthesizing carboxylic acids and their derivatives. Although there has been impressive progress in transition-metal-catalyzed CO<sub>2</sub> functionalization of C(sp<sup>2</sup>)-H bonds,<sup>[36]</sup> direct carboxylation of unactivated C(sp<sup>3</sup>)-H bonds remains challenging. Numerous light-promoted carboxylation reactions of C(sp<sup>3</sup>)-H have



##### Selected substrates



##### Proposed mechanism



**Scheme 13.** Photocarboxylation of benzylic C(sp<sup>3</sup>)-H bonds and the proposed mechanism.

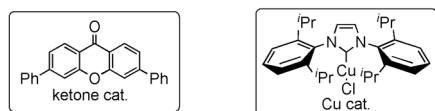
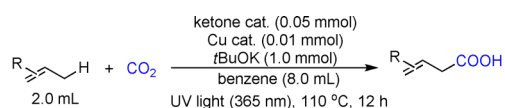
recently been developed to tackle this challenge. In 2015, Murakami and co-workers disclosed the first carboxylation of benzylic C(sp<sup>3</sup>)-H bonds of *ortho*-alkylphenyl ketones promoted by UV or sunlight (Scheme 13).<sup>[37]</sup> A variety of aryl compounds (including an aryl aldehyde **81d**) were well tolerated with moderate to good yields. It was proposed that the excited diaryl carbonyl group could abstract a hydrogen atom from the *o*-methyl group to yield a biradical species **84**. This biradical species will presumably undergo rearrangement and endergonic isomerization to generate a highly reactive *o*-quinone methide **85** through a Norrish type II pathway. A subsequent [4+2] cycloaddition between the *E*-isomer of **85** and CO<sub>2</sub> affords a six-membered cycloadduct **86**, which undergoes a ring-opening to provide the desired acid **87**. The *Z*-isomer, on the other hand, would undergo a 1,5-hydrogen atom shift to regenerate the starting material. It is worth noting that sunlight can effectively promote this transformation.

In 2016, Murakami et al. reported a photo-induced carboxylation reaction of allylic C-H bonds using CO<sub>2</sub> and a combination of an aryl ketone type photocatalyst and a copper carboxylation catalyst under UV light irradiation (Scheme 14).<sup>[38]</sup> Both acyclic and cyclic alkenes were tolerated in the reaction, providing the corresponding carboxylic acids. However, it was observed that unsymmetrical alkenes containing two distinct types of C-H bonds at the allylic positions afforded mixtures of isomers (**89d** and **89e**).

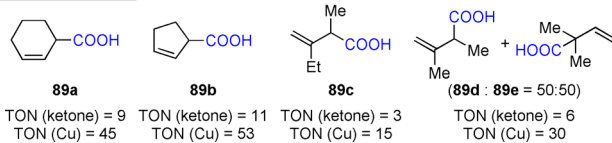
Mechanistically, photocatalyst **90** is excited by UV light to generate an excited state **91**, inducing an intermolecular HAT process between **91** and the allylic substrate to generate a transient radical pair species **92** (Scheme 15). This radical pair would presumably undergo a radical-radical coupling reaction, producing the tertiary homoallylic alcohol intermediate **93**. Subsequent deprotonation of **94** by copper *tert*-butoxide and C-C bond-cleaving reaction through  $\beta$ -carbon elimination yield the allylcopper species **95**. A nucleophilic addition of **95** to CO<sub>2</sub> generates **96**, which undergoes ligand



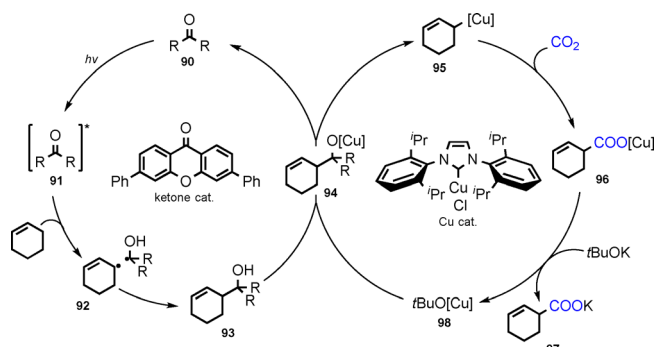




## Selected substrates



**Scheme 14.** Photo-induced carboxylation of allylic C–H bonds of simple alkenes.

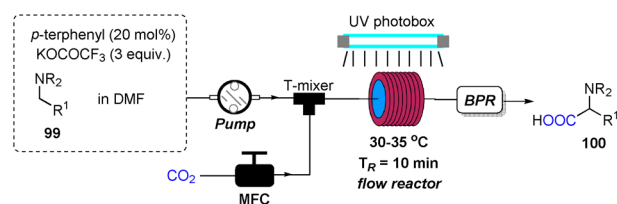


**Scheme 15.** Proposed mechanism of photo-induced carboxylation of allylic C–H bonds of simple alkenes.

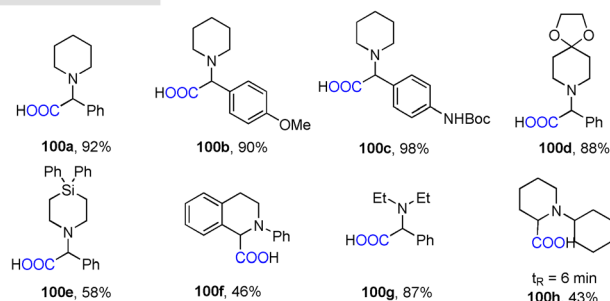
exchange with potassium *tert*-butoxide to afford product **97** as the potassium salt, and regenerates the copper catalyst **98**.

In 2016, Jamison and co-workers developed a novel continuous-flow method using CO<sub>2</sub> and amines to synthesize  $\alpha$ -amino acids under UV light irradiation (Scheme 16 A).<sup>[39]</sup> A wide range of benzyl amines with different functionalities were tolerated in the reaction, affording a variety of amino acids **100 a–100 g** in good yields. High regioselectivity favoring the benzylic carboxylation was observed and non-benzylic amines with less activated  $\alpha$ -amino C–H bonds, such as *N*-cyclohexylpiperidine, selectively yielded an amino acid product **100 h** with moderate yields. The free amino acid could be obtained by cleavage of the 4-piperidone protecting group under neutral conditions, employing a polymer-supported amine scavenger such as JandaJel-NH<sub>2</sub> (Scheme 16 B).

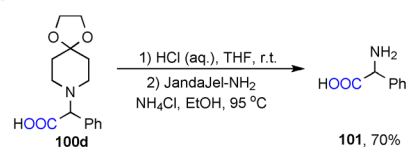
It was proposed that the excited singlet state of *p*-terphenyl **102** is generated by irradiation of *p*-terphenyl with UV light (Scheme 17). A subsequent SET between **102** and the tertiary amine **99** produces the strongly reducing *p*-terphenyl radical anion **103** and the corresponding amine radical cation **105**. The radical anion **103** then donates an electron to CO<sub>2</sub> to form a CO<sub>2</sub> radical anion **104**. In the meantime, deprotonation of amine radical cation **105** gives a neutral amine radical **106**, which after a radical-radical coupling with CO<sub>2</sub> radical anion **104** and subsequent protonation affords the carboxylic acid **100**.

A)  $\alpha$ -Amino acids synthesis

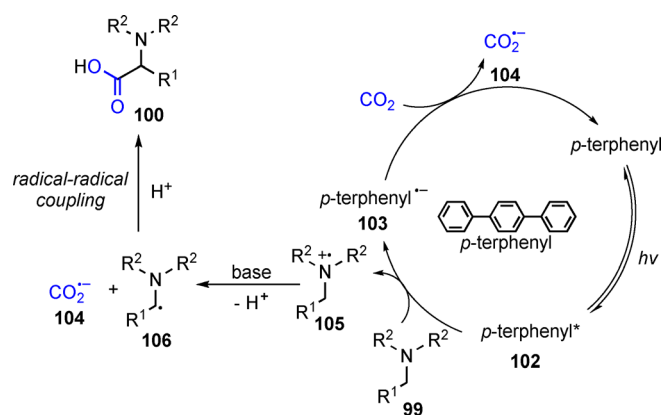
## Selected substrates



## B) Protecting group removal



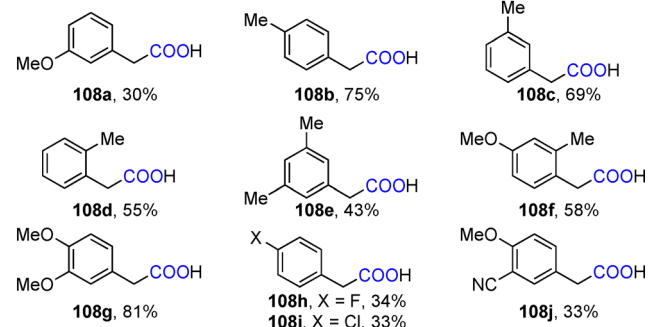
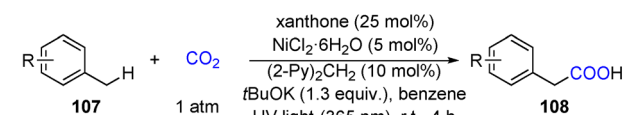
**Scheme 16.** a) Syntheses of  $\alpha$ -amino acids utilizing CO<sub>2</sub> and amines in continuous-flow reactors irradiated by UV light; b) Synthesis of the free amino acid can be achieved via the deprotection of a piperidone derivative. MFC=mass flow controller; BPR=back pressure regulator.



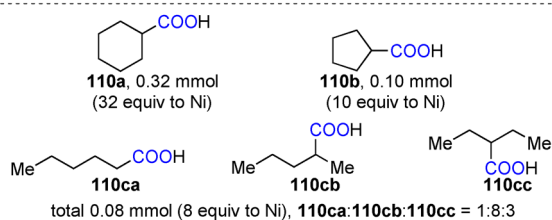
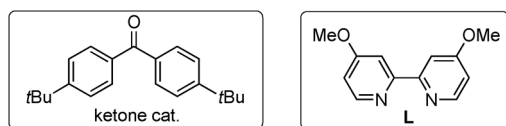
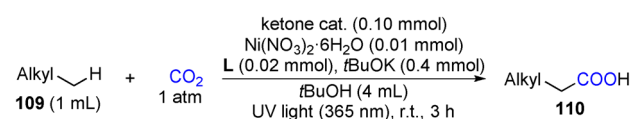
**Scheme 17.** Proposed mechanism of the synthesis of  $\alpha$ -amino acids utilizing CO<sub>2</sub> and amines in continuous-flow reactors irradiated by UV light.

In 2019, Murakami and co-workers reported a UV light-promoted carboxylation of benzylic and aliphatic C–H bonds via ketone/Ni dual catalysis.<sup>[40]</sup> Various substituted benzene derivatives were carboxylated at the benzylic positions (Scheme 18 A). This methodology was also effective in the carboxylation of simple alkanes such as cyclohexane, cyclopentane, and pentane, although a mixture of three regioisomers was generated when *n*-pentane was the alkane substrate (Scheme 18 B).

## A) Carboxylation of methylbenzene derivatives

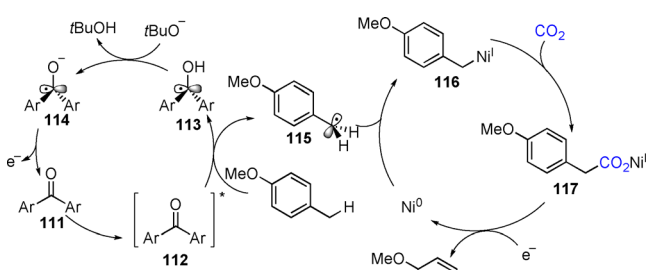


## B) Carboxylation of hydrocarbons



**Scheme 18.** UV light-promoted carboxylation of benzylic and aliphatic C–H bonds with CO<sub>2</sub> via ketone/nickel dual catalysis.

In the proposed mechanism, a ketone is excited by UV light (Scheme 19). The excited ketone **112** is able to abstract the H atom from benzylic or aliphatic C(sp<sup>3</sup>)–H bonds producing a ketyl radical **113** and a benzylic or aliphatic radical **115**. The ketyl radical **113** is deprotonated by *t*BuO<sup>−</sup> to give a ketyl radical anion **114**, which is able to reduce the Ni<sup>II</sup> precursor to Ni<sup>0</sup>. The benzylic radical or aliphatic radical

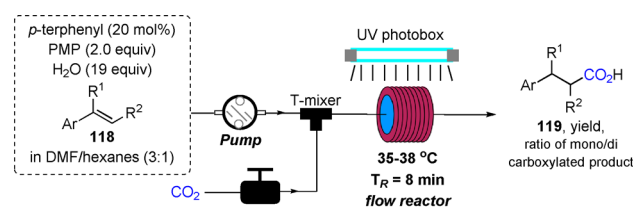


**Scheme 19.** Mechanism of UV light-promoted ketone/nickel dual catalytic carboxylation of C(sp<sup>3</sup>)–H bonds.

formed (**115**) is captured by Ni<sup>0</sup> to form a Ni<sup>I</sup> complex **116**. Insertion of CO<sub>2</sub> into C–Ni<sup>I</sup> gives a Ni<sup>I</sup> carboxylate species **117**, which is reduced by ketyl radical anion to produce the carboxylate and regenerate the Ni<sup>0</sup> catalyst.

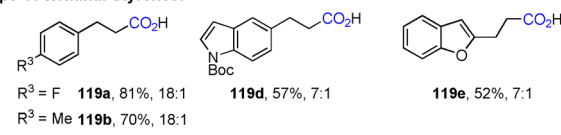
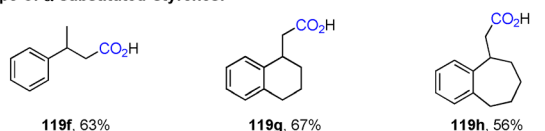
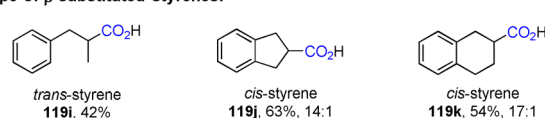
## 3.1.2. UV Light-Promoted Carboxylation of Alkenes with Carbon Dioxide

Continuous-flow  $\beta$ -selective hydrocarboxylation of styrenes was demonstrated by Jamison et al., employing 1,2,2,6,6-penta-methylpiperidine (PMP) as a reductant under UV light irradiation (Scheme 20). In this catalytic system, the photo-excited *p*-terphenyl catalyst ( $E^0 = -2.63$  V vs. SCE in DMF) undergoes a SET with PMP to yield a strongly reducing *p*-terphenyl radical anion and a PMP radical cation.<sup>[41]</sup> CO<sub>2</sub> is reduced to the corresponding radical anion ( $E^0 = -2.21$  V vs. SCE in DMF) by the *p*-terphenyl radical anion **122**. The CO<sub>2</sub> radical anion **104** then attacks the  $\beta$ -position of the styrene, producing a stable benzylic radical **120**. The benzylic radical **120** can then be reduced by the photocatalytic cycle to yield

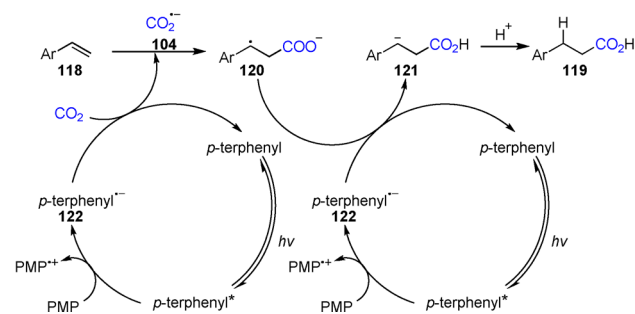


## Selected substrates

## Scope of terminal styrenes:

Scope of  $\alpha$ -substituted styrenes:Scope of  $\beta$ -substituted styrenes:

## Proposed mechanism



**Scheme 20.** Selective  $\beta$ -carboxylation of styrenes in continuous-flow reactors.



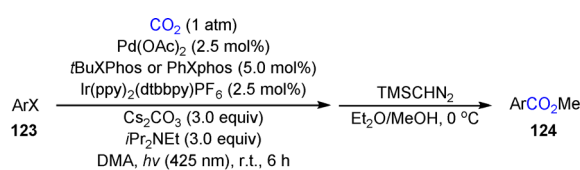
a carbanion **121**, which is protonated to yield the desired dicarboxylated product. Notably, the reaction tolerates both  $\alpha$ - and  $\beta$ -substituted styrenes selectively providing the  $\beta$ -carboxylated products **119** in moderate yields. The reaction time required to complete this transformation can be reduced to 8 min by taking advantage of the continuous-flow apparatus.

### 3.2. Visible-Light-Promoted Carboxylation with Carbon Dioxide

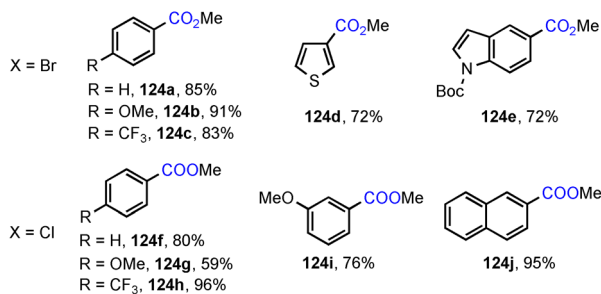
#### 3.2.1. Visible-Light-Promoted Carboxylation of C–Halogen Bonds and Their Equivalents

The carboxylation of C–halogen bonds provides a facile and straightforward method with which to introduce carboxylate functionalities. Early studies by Yamamoto et al. in the field of transition-metal-mediated carboxylation demonstrated that  $\text{PhNi(L)Br}$  ( $L = \text{bipyridine}$ ) can react with  $\text{CO}_2$  to generate benzoic acids in moderate yields.<sup>[42]</sup> Significant advances were made by Martin and co-workers in 2009,<sup>[43]</sup> who reported the first catalytic carboxylation of alkyl bromides.<sup>[44]</sup> However, a stoichiometric amount of organometallic reductants was required in this transformation. In 2017, Iwasawa and co-workers reported the first example of visible-light-mediated carboxylation of aryl halides with  $\text{CO}_2$  using catalytic amount of  $\text{Pd(OAc)}_2$  and  $\text{Ir(ppy)}_2(\text{dtbbpy})\text{PF}_6$  as a photoredox catalyst and  $N,N$ -diisopropylethylamine ( $i\text{Pr}_2\text{NEt}$ ) as a stoichiometric reductant, thereby overcoming the need for stoichiometric organometallic reductants (Scheme 21).<sup>[45]</sup> Various arylbromides (**123 a–123 e**) and chlorides (**123 f–123 j**) with different steric and electronic environments and heteroatoms could be used in this protocol to afford carboxylation products **124** with moderate to excellent yields.

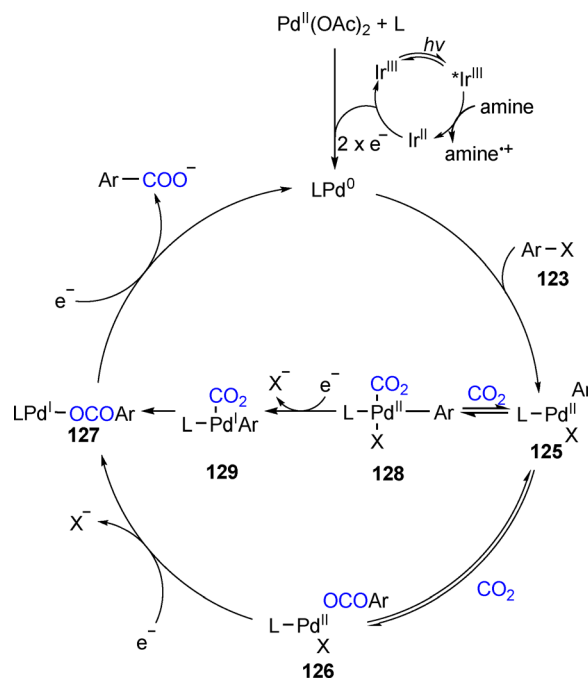
It was proposed that the reaction is initiated by the reductive quenching of the excited photocatalyst by  $i\text{Pr}_2\text{NEt}$  to yield an amine radical cation and reduced  $\text{Ir}^{\text{II}}$  species (Scheme 22). Subsequent reduction of the  $\text{Pd}^{\text{II}}$  complex by  $\text{Ir}^{\text{II}}$



#### Selected substrates



**Scheme 21.** Visible light-mediated Pd-catalyzed carboxylation of aryl halides.



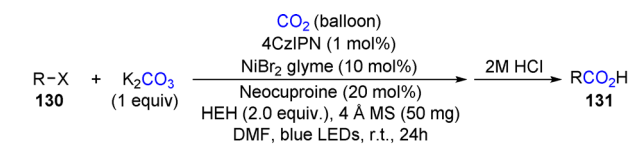
**Scheme 22.** Proposed mechanism of visible light-mediated Pd-catalyzed carboxylation of aryl halides.

via single electron reduction generates the active  $\text{Pd}^0$  species, which undergoes an oxidative addition with aryl halides **123** to yield a  $\text{Pd}^{\text{II}}$  complex **125**. The insertion of  $\text{CO}_2$  into the Ar–Pd bond in **125** may occur before or after the single electron reduction of  $\text{Pd}^{\text{II}}$  to produce either **126** or **128**. Both proposed pathways however lead to the formation of  $\text{Pd}^{\text{I}}$  carboxylate species **127**, which undergoes a further single electron reduction to obtain the product and regenerate the  $\text{Pd}^0$  species.

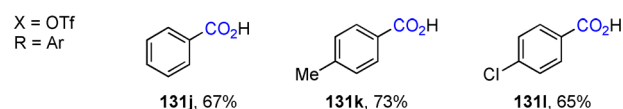
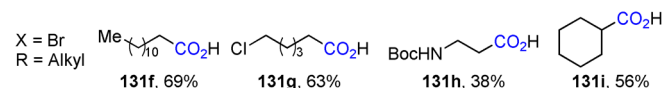
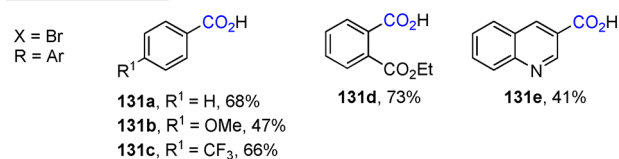
König and co-workers later reported the carboxylation of aromatic and aliphatic bromides and triflates with  $\text{CO}_2$  (Scheme 23).<sup>[46]</sup> In this reaction, Ni was used as the transition metal catalyst and  $4\text{CzIPN}$  was employed as the photocatalyst. Hantzsch ester (HEH) was employed as a reductant while  $\text{K}_2\text{CO}_3$  served as the  $\text{CO}_2$  source. The reaction displayed a broad substrate scope. Aryl- and alkyl- bromides and aryl triflates performed well in this reaction, generating carboxylic acids **131** in moderate to excellent yields. Notably, primary alkyl bromides, including *tert*-butoxycarbonyl (Boc) protected amines, can react effectively to yield the corresponding acid products **131h**. In addition, unactivated cyclic alkyl bromides can be converted to the corresponding acid products **131i** in moderate yield by adding one equivalent of cesium fluoride ( $\text{CsF}$ ).

Similarly, the groups of Iwasawa and Jana separately described the carboxylation of aryl triflates with  $\text{CO}_2$  by using Pd/Ir dual catalytic systems under visible-light irradiation.<sup>[47]</sup> Carboxylation of alkenyl triflates was also achieved under Iwasawa's conditions with a relatively short reaction time.

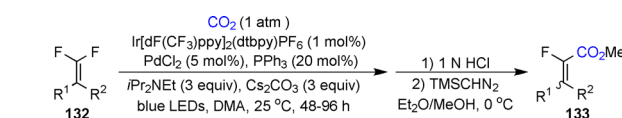
In 2019, the Feng group demonstrated the selective carboxylation of *gem*-difluoroalkenes through photoredox/Pd dual catalysis (Scheme 24).<sup>[48]</sup> A variety of aryl difluoroalkenes were evaluated to furnish predominantly *Z*- $\alpha$ -fluoro-



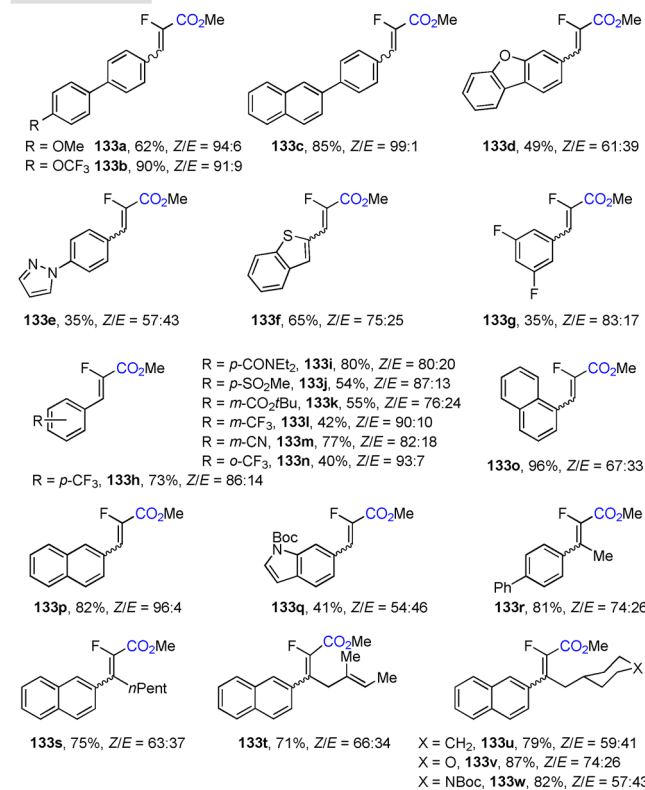
## Selected substrates



**Scheme 23.** Visible light mediated Ni-catalyzed carboxylation of aryl and aliphatic halides.



## Selected substrates

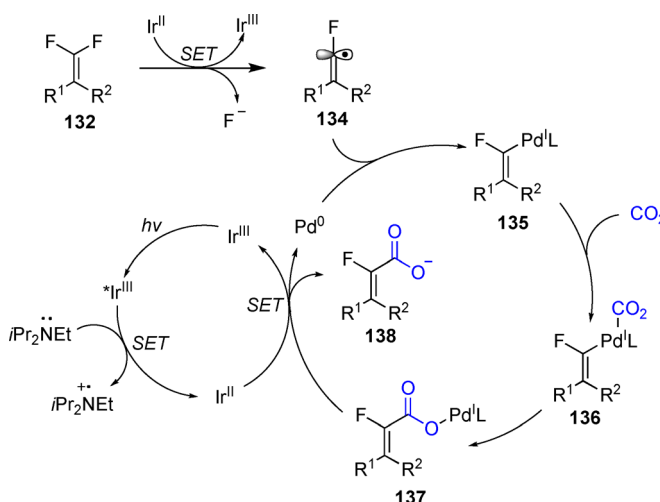


**Scheme 24.** Selected substrate scope for defluoro carboxylation.

crylic acids **133** in moderate to good yields, while alkyldifluoroalkenes failed to couple with CO<sub>2</sub>. The reaction displayed good functional group compatibility, tolerating

dibenzofuran (**133d**), benzothiophene (**133f**) and indole (**133q**) moieties.

Mechanistically, the reaction is initiated by a SET between *i*Pr<sub>2</sub>NEt and the photo-excited photocatalyst to produce the reduced photocatalyst Ir<sup>II</sup>, which reduces the *gem*-difluoroalkene **132** to yield fluoroalkenyl radical **134** (Scheme 25). The carbon radical **134** is intercepted by Pd<sup>0</sup> to form a putative Pd<sup>I</sup> species **135**, representing a rare example in which a transition metal is employed to intercept the fluorine-containing carbon radical to form a versatile organometallic species. Subsequent CO<sub>2</sub> coordination and migratory insertion with **136** affords a carboxyl-Pd<sup>I</sup> complex **137**. A SET between **137** and Ir<sup>II</sup> photocatalyst regenerates Pd<sup>0</sup> and yields the carboxylate **138**.

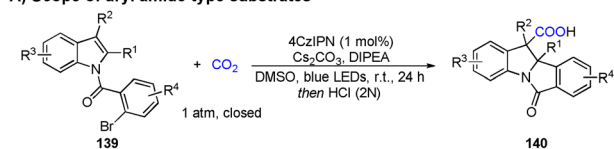


**Scheme 25.** Proposed mechanism for defluoro carboxylation.

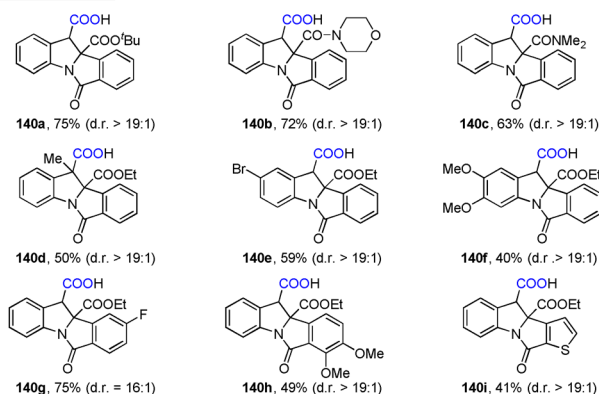
Yu and co-workers recently developed a dearomative arylcarboxylation of indoles with CO<sub>2</sub> which selectively produces indoline-3-carboxylic acids by a successive single-electron transfer (SSET) strategy (Scheme 26).<sup>[49]</sup> Under transition-metal catalysis, the dearomative reductive coupling of indoles with two electrophiles is challenged by the low reactivity of the aromatic carbon-carbon double bond. It was proposed that these challenges could be overcome by using a radical relay SSET strategy. The authors envisioned that the reduction of the carbon-halide bond by visible-light-induced single-electron transfer would lead to a highly reactive aryl radical which would then undergo a selective intramolecular radical addition to the C2–C3 double bond in indoles instead of CO<sub>2</sub>. Subsequent SET would reduce the benzylic radical to a benzylic anion, which after trapping with CO<sub>2</sub> and protonation would produce the arylcarboxylation product. Indeed, after reaction optimization, this transformation exhibited a broad substrate scope and high chemo- and diastereoselectivity. Substrates bearing functional groups such as bromo (**140e**), fluoro (**140g**) and thiophene (**140i**) were well tolerated (Scheme 26A). Notably, an all-carbon quaternary center could be formed to deliver product **140d** with high diastereoselectivity. For unactivated aryl halides (Scheme 26B), with modified conditions, various aryl bromides



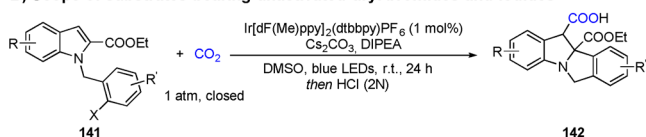
## A) Scope of aryl amide type substrates



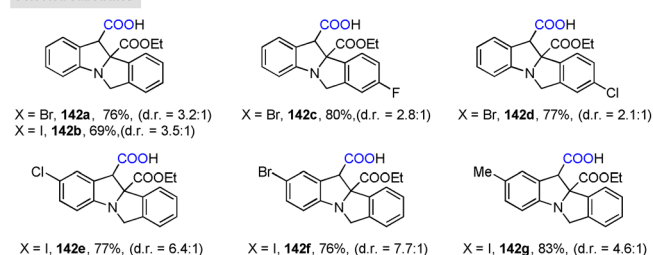
## Selected substrates



## B) Scope of substrates bearing unactivated aryl bromides and iodides



## Selected substrates

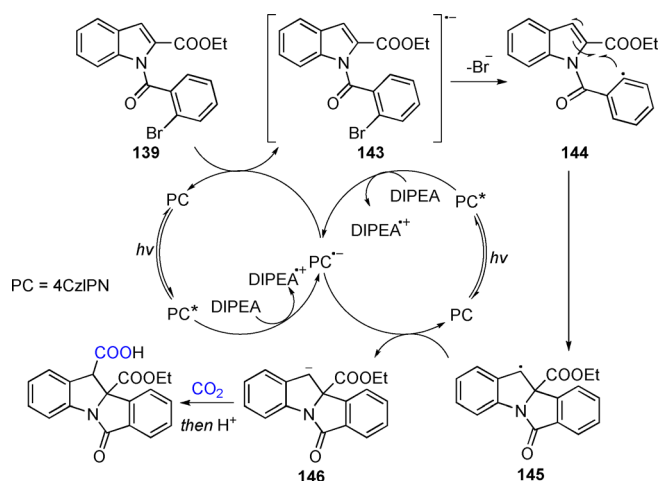


Scheme 26. Reductive dearomative difunctionalization of indoles.

and iodides could proceed the reaction effectively, albeit with reduced diastereoselectivity.

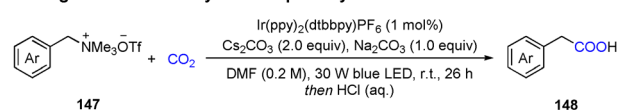
In light of these experiments, a possible mechanism was proposed (Scheme 27). Radical anion  $4CzIPN^{\cdot-}$  and the radical cation  $DIPEA^{\cdot+}$  are generated by reductive quenching of the photo-excited  $4CzIPN$  ( $E_{1/2} [4CzIPN^{\cdot-}/4CzIPN^*] = +1.35$  V vs. SCE in MeCN) by  $DIPEA$  ( $E_{1/2}^{ox} = +0.63$  V vs. SCE in DMF). An arylbromide **139** is reduced by a single electron transfer from  $4CzIPN^{\cdot-}$  to generate the radical anion **143**. Subsequent fragmentation of **143** releases a bromide anion to give an aryl radical **144**, which undergoes an intramolecular radical addition to the C2–C3 double bond of indole to deliver the benzylic radical **145**. A second single electron transfer from  $4CzIPN^{\cdot-}$  to **145** leads to the formation of a carbon anion **146**, which undergoes nucleophilic addition to  $CO_2$  followed by protonation to deliver the desired dearomative arylcarboxylation product.

The Yu group disclosed the first external reductant-free visible-light-driven carboxylations of organic tetraalkyl ammonium salts with  $CO_2$  (Scheme 28).<sup>[50]</sup> The cross-electrophile coupling tolerates primary, secondary and tertiary C–N bonds and a variety of functional groups, giving  $\alpha$ -substituted aryl

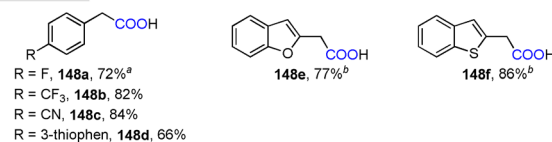


Scheme 27. Plausible mechanism for the arylcarboxylation of indoles.

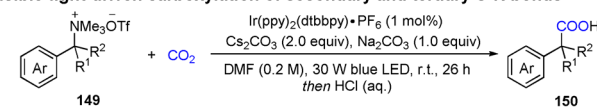
## A) Visible-light-driven carboxylation of primary C–N bonds



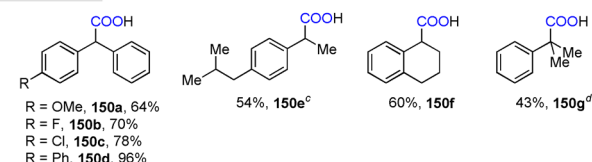
## Selected substrates



## B) Visible-light-driven carboxylation of secondary and tertiary C–N bonds



## Selected substrates

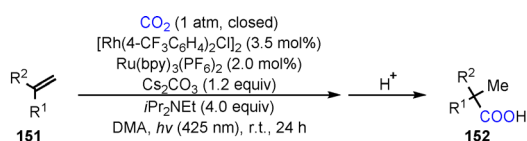
Scheme 28. Visible-light-driven carboxylation of C–N bonds. <sup>a</sup> [Ir]-catalyst (3 mol %),  $Na_2HPO_4$  instead of  $Na_2CO_3$ , 36 h. <sup>b</sup> [Ir]-catalyst (3 mol %), 36 h. <sup>c</sup> [Ir]-catalyst (4 mol %). <sup>d</sup>  $K_2CO_3$  instead of  $Na_2CO_3$ .

acetic acids **148** in moderate to good yields. TEMPO trapping experiments indicated the involvement of radicals. In addition, a control experiment with  $D_2O$  as the additive demonstrated the HAT with solvent (DMF) and the formation of a benzylic anion intermediate. Moreover, the reaction with deuterated substrates indicated that the amine radical cation deprotonation and benzylic anion protonation occurs during the reaction process. Stern–Volmer luminescence studies and electrochemical analysis suggested that the iridium catalyst might be quenched by  $NMe_3$  generated in situ from the ammonium salt or an  $\alpha$ -amino radical. Moreover, the presumed benzyl radical ( $E_{1/2}^{red} = -1.43$  V vs. SCE) might undergo further reduction by  $Ir^{II}$ -catalyst [ $E_{1/2}^{red} (Ir^{III}/Ir^{II}) = -1.51$  V vs. SCE] to afford a benzylic carbon anion. The subsequent nucleophilic attack of the carbon anion to  $CO_2$

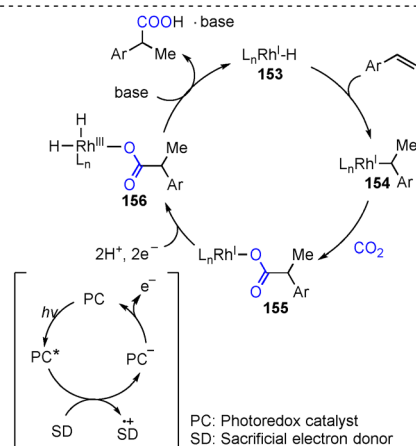
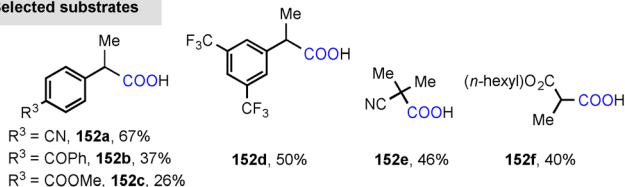
and protonation gave the carboxylic acid products. However, the authors could not exclude other alternative pathways, including the coupling between benzyl radicals and ketyl radicals.

### 3.2.2. Visible-Light-Promoted Carboxylation of Alkenes with Carbon Dioxide

Pioneering studies from Hoberg et al. demonstrated the light-mediated formation of five-membered nickelacycles from Ni<sup>0</sup>, alkenes and CO<sub>2</sub>. Encouraged by Hoberg's work,<sup>[51]</sup> the Rovis group reported the first Ni-catalyzed hydrocarboxylation of aryl alkenes using a stoichiometric amount of ZnEt<sub>2</sub> as the reductant.<sup>[52]</sup> Subsequently, several other groups demonstrated the use of various complexes of transition metals such as Fe, Rh and Ru as suitable catalysts for hydrocarboxylation of olefins.<sup>[53]</sup> In 2017, Iwasawa and co-workers disclosed the first visible-light-driven catalytic hydrocarboxylation of alkenes with CO<sub>2</sub> using a combination of a Rh complex as a carboxylation catalyst and a [Ru(bpy)<sub>3</sub>]<sup>2+</sup> photocatalyst in the presence of a tertiary amine (Scheme 29).<sup>[54]</sup> The substrate scope was limited to only electron-deficient styrenes, which yielded products **152** in moderate yields. Mechanistically, the authors were able to prove that the reductant, *i*Pr<sub>2</sub>NEt, could serve as a proton source to form the key Rh-hydride intermediate under photoredox conditions. Control experiments revealed that the photoredox catalyst, light and the tertiary amine were all essential for the carboxylation reaction. A luminescence quenching study showed that



#### Selected substrates

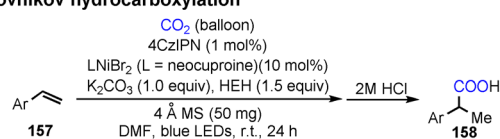


**Scheme 29.** Visible-light-driven Rh-catalyzed hydrocarboxylation of alkenes.

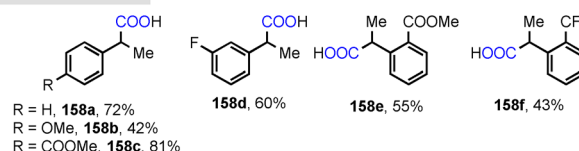
a triplet-triplet energy transfer process could be involved in the carboxylation. The key catalytic species, the Rh<sup>I</sup> complex **153** undergoes hydrometallation and nucleophilic carboxylation to yield the Rh<sup>I</sup> carboxylate complex **155**. Complex **155** then undergoes electron and proton transfers enabled by the photoredox catalyst to generate a Rh<sup>III</sup> dihydride **156**, which delivers the carboxylic acid in the presence of a base and regenerates complex **153**.

König and co-workers developed a regioselective hydrocarboxylation of aryl alkenes using CO<sub>2</sub> via the synergistic merger of a photoredox catalyst with a nickel catalyst (Scheme 30).<sup>[55]</sup> The regioselectivity of this reaction is dependent on the choice of the ligand. The use of neocuproine as ligand yielded the Markovnikov products **158** (branched:linear = 100:1) (Scheme 30A), while the use of 1,4-bis-(diphenylphosphino)butane (dppb) as ligand promoted the formation of anti-Markovnikov products **159** (Scheme 30B).

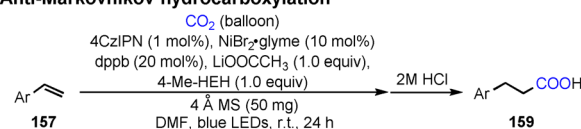
#### A) Markovnikov hydrocarboxylation



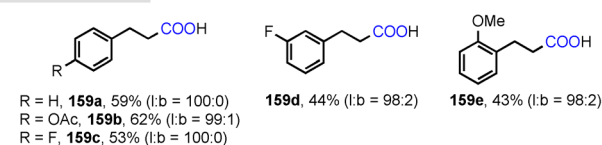
#### Selected substrates



#### B) Anti-Markovnikov hydrocarboxylation



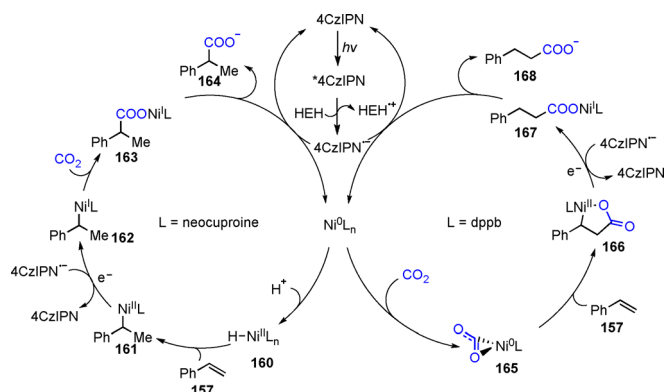
#### Selected substrates



**Scheme 30.** Visible-light-driven Ni-catalyzed regioselective hydrocarboxylation of aryl alkenes.

Based on the proposed mechanism (Scheme 31), the active Ni<sup>0</sup> [ $E_{1/2}^{\text{red}}(\text{Ni}^{\text{II}}/\text{Ni}^0) = -1.2$  V vs. SCE] species is generated from Ni<sup>II</sup> in situ via two single electron transfer steps under photocatalytic reductive conditions [4CzIPN<sup>-</sup> ( $E_{1/2}^{\text{red}} = -1.21$  V vs. SCE)]. When neocuproine is used as the ligand, protonation by the Hantzsch ester radical cation produced a Ni hydride complex **160**. Ni hydride **160** then undergoes hydrometallation with styrene, yielding an organo-nickel complex **161**. Reduction of the complex followed by the insertion of CO<sub>2</sub> leads to the generation of a nickel carboxylate intermediate **163**. Further reduction of **163** gives the Markovnikov product. On the other hand, when dppb is employed, a five-membered nickelacycle **166** is generated

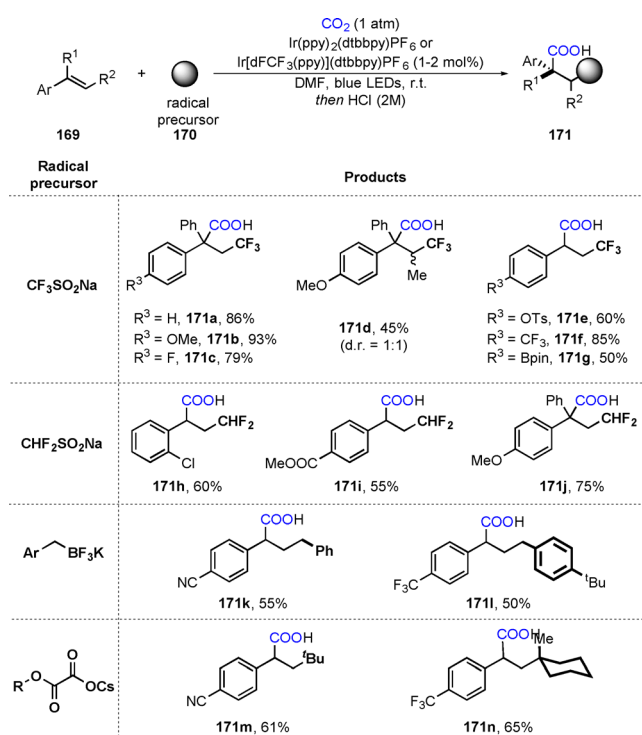




**Scheme 31.** Proposed mechanism of visible light driven Ni-catalyzed regioselective hydrocarboxylation of aryl alkenes.

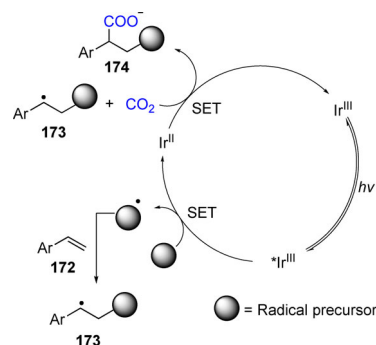
through the formation of complex **165**. The nickelacycle **166** can subsequently be reduced to yield a Ni<sup>I</sup> complex **167**. Finally, single electron reduction of **167** affords the anti-Markovnikov product and regenerates the Ni<sup>0</sup> catalyst.

Compared to hydrocarboxylation of alkenes, difunctionalization of alkenes using CO<sub>2</sub> is more challenging and provides products with higher structural diversity. In this context, Martin and co-workers reported the first example of visible-light-promoted, photoredox-catalysis assisted difunctionalization of alkenes with CO<sub>2</sub> (Scheme 32).<sup>[56]</sup> In their study, the authors demonstrated a redox-neutral intermolecular dicarbofunctionalization of styrenes with CO<sub>2</sub> and simple radical precursors, such as sulfonates including the Langlois reagent (CF<sub>3</sub>SO<sub>2</sub>Na), trifluoroborates and oxalates without requiring stoichiometric reductants. Notably, the merits of the



**Scheme 32.** Dicarbofunctionalization of styrenes with CO<sub>2</sub>.

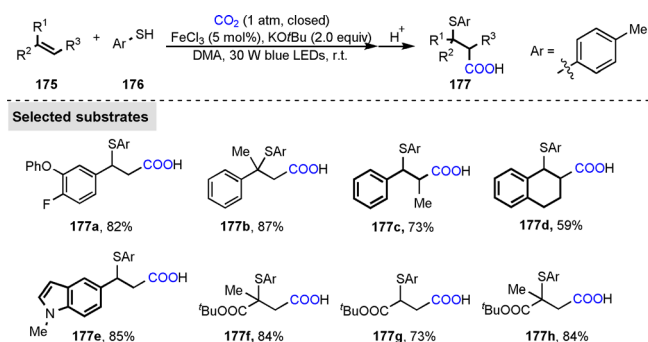
trifluoromethylcarboxylation were demonstrated by its tolerance of wide range of sensitive functional groups, including tosylates (**171e**) and boronic esters (**171g**). Mechanistically, the reaction is thought to proceed through a radical generated by single electron reduction with the excited photocatalyst Ir(ppy)<sub>2</sub>(dtbbpy)PF<sub>6</sub> [ $E_{1/2}^{\text{red}}(\text{Ir}^{\text{III}}/\text{Ir}^{\text{II}}) = -1.51 \text{ V vs. SCE}$  in MeCN] adding to the vinyl arene **172** to form a benzylic radical **173**. Another single electron reduction of radical **173** would generate a benzylic anion, which finally traps CO<sub>2</sub> to yield the carboxylate **174** (Scheme 33). Li's group utilized



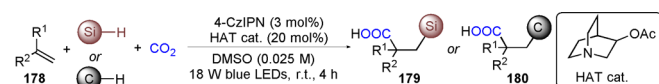
**Scheme 33.** Proposed mechanism of dicarbofunctionalization of styrenes with CO<sub>2</sub>.

perfluoroalkyl iodides as radical precursors to achieve a visible-light-driven carboxylative cyclization of allyl amines to give perfluoroalkylated oxazolidinones in the presence of CO<sub>2</sub> and a base.<sup>[57]</sup> Yu et al. further expanded the reaction scope to difluoroalkyl bromides assisted by photoredox catalysis.<sup>[58]</sup> In 2019, Cheng's group reported a palladium-catalyzed radical carboxylative cyclization of 2-(1-arylviny)anilines to generate 1,4-dihydro-2H-3,1-benzoxazin-2-ones using alkyl bromides and CO<sub>2</sub> under visible-light irradiation.<sup>[59]</sup>

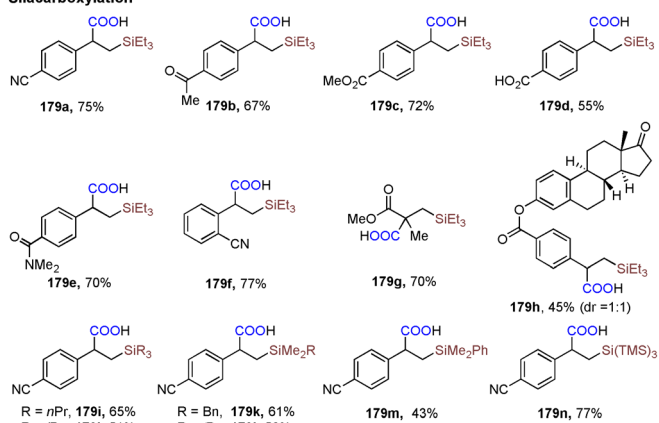
A visible-light-promoted, iron-catalyzed thiocarboxylation of styrenes and acrylates with CO<sub>2</sub> was reported in 2017 by the Yu group (Scheme 34).<sup>[60]</sup> A range of styrenes and acrylates could be employed in this system to give useful  $\beta$ -thioacids **177** in good yields with high regio-, chemo- and diastereo-selectivity. The precise mechanism was not fully clear, but the authors proposed that CO<sub>2</sub> radical anion and alkyl radicals might be involved in the catalytic cycle to achieve this unique regioselectivity.



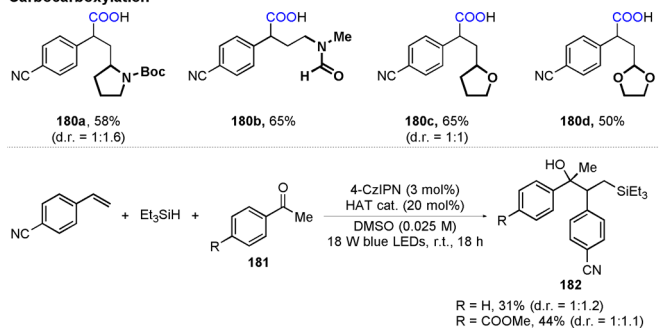
**Scheme 34.** Thiocarboxylation of styrenes and acrylates.



## Silacarboxylation



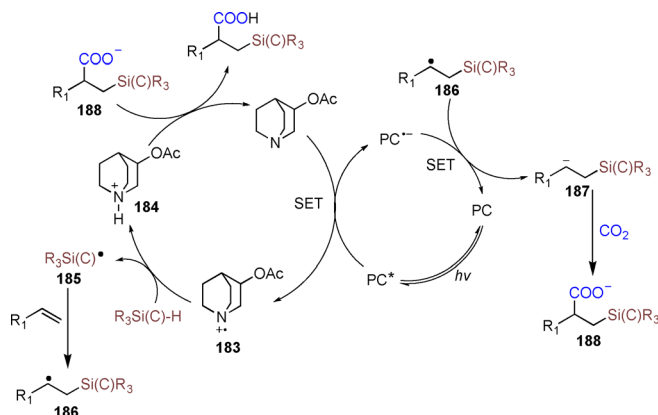
## Carbocarboxylation



**Scheme 35.** Silacarboxylation and carbocarboxylation of styrenes and acrylates.

Wu and co-workers developed a three-component metal-free silacarboxylation and carbocarboxylation between electron-deficient alkenes, CO<sub>2</sub> and either silanes or C(sp<sup>3</sup>)-H alkanes through a synergistic combination of photoredox and HAT catalysis (Scheme 35).<sup>[61]</sup> The silacarboxylation tolerates a variety of functional groups including cyano (**179a**), ketone (**179b**), carboxylic acid (**179d**) and amide (**179e**) groups, producing β-silacarboxylic acids in moderate to good yields. The synthetic application of this protocol was also demonstrated in the late-stage elaboration of a biologically relevant complex molecule **179h**. Common silanes such as tripropylsilane, triisopropylsilane, dimethylbenzylsilane, dimethyltert-butylsilane, and dimethylphenylsilane were viable in this transformation. The strategy was also successfully extended to carbocarboxylation, where excellent functional group compatibility was illustrated, giving products such as γ-amino acids (**180a**, **180b**) which are important structural motifs in many pharmaceutically important compounds. Notably, aryl ketones could be used as electrophiles in a three-component coupling reaction with silanes and alkenes to produce γ-silyl alcohols **182**.

The mechanism was proposed to begin with the photo-activation of 4CzIPN to 4CzIPN\* (Scheme 36). 4CzIPN\* would then be reductively quenched by 3-acetoxyquinuclidine, yielding reduced 4CzIPN<sup>-</sup> and a radical cation inter-



**Scheme 36.** Proposed mechanism for silacarboxylation and carbocarboxylation of styrenes and acrylates.

mediate **183**. This radical cation **183** promotes a HAT from Si-H or C-H to generate a silyl or carbon radical **185** and a quinuclidinium cation **184**. The generated silyl or carbon radical **185** adds to the alkene to yield radical intermediate **186** (-0.77 V vs. SCE for *p*-CN benzyl radical analogue), which is then reduced by the 4CzIPN<sup>-</sup> ( $E_{1/2}^{\text{red}} = -1.21$  V vs. SCE in MeCN) to generate an anion **187**. The anion **187** subsequently undergoes nucleophilic addition to carbon dioxide and protonation to yield the desired silacarboxylation or carbocarboxylation product.

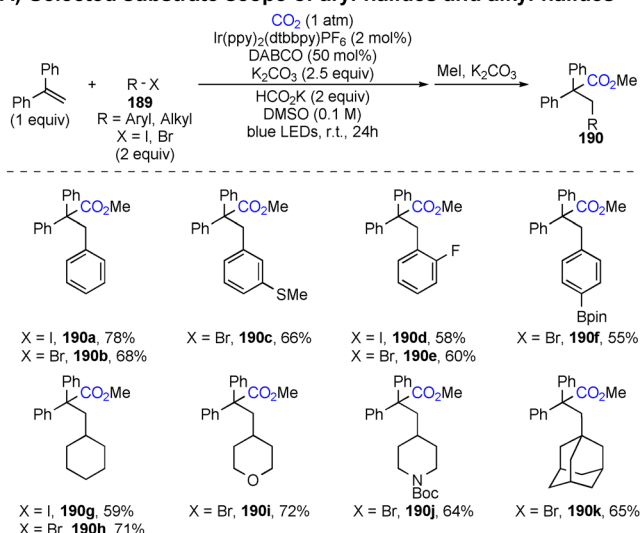
Inspired by the recent efforts in the development of alkene difunctionalization, Li and co-workers developed a visible-light-driven reductive carboarylation of styrenes with CO<sub>2</sub> and aryl halides in a regioselective manner using the readily available and inexpensive HCO<sub>2</sub>K as the terminal reductant (Scheme 37).<sup>[62]</sup> This method provided an atom-economic and direct access to valuable hydrocinnamic acid derivatives **190**. The reaction exhibits a broad substrate scope of aryl iodides, bromides, with good yields and excellent regioselectivity (Scheme 37A). Moreover, a variety of (hetero)aryl moieties were well tolerated, affording products **193** with moderate to good yields (Scheme 37B). Less reactive aryl chlorides were effective in this reaction and the substrate scope can also be extended to alkyl halides. In addition, substituted styrenes were more effective than α,β-unsubstituted styrene derivatives, while aliphatic alkenes were unreactive. By employing <sup>13</sup>C labeling, it was found that 74% of <sup>13</sup>C incorporation was from CO<sub>2</sub> gas with the rest of the CO<sub>2</sub> source being derived from HCO<sub>2</sub>K or K<sub>2</sub>CO<sub>3</sub>.

A plausible mechanism was proposed based on all the experimental results and literature precedents (Scheme 38). The photo-excited \*Ir<sup>III</sup> is produced upon blue light irradiation, which is subsequently reductively quenched by 1,4-diazabicyclo[2.2.2]octane (DABCO) to give Ir<sup>II</sup> and a radical cation of DABCO. A hydrogen atom transfer from HCO<sub>2</sub>K promoted by DABCO radical cation gives a CO<sub>2</sub> radical anion, which reduces aryl halide to an aryl radical **194**. Subsequent regioselective addition of this aryl radical to alkene affords a benzylic radical **195**, which is further reduced by Ir<sup>II</sup> to a benzylic anion **196**. Nucleophilic addition of **196** to CO<sub>2</sub> produces the carboxylate **197**, which is methylated to deliver an ester product.

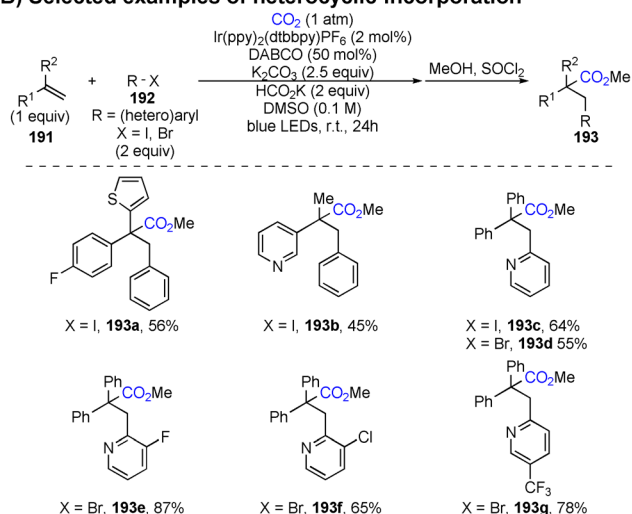




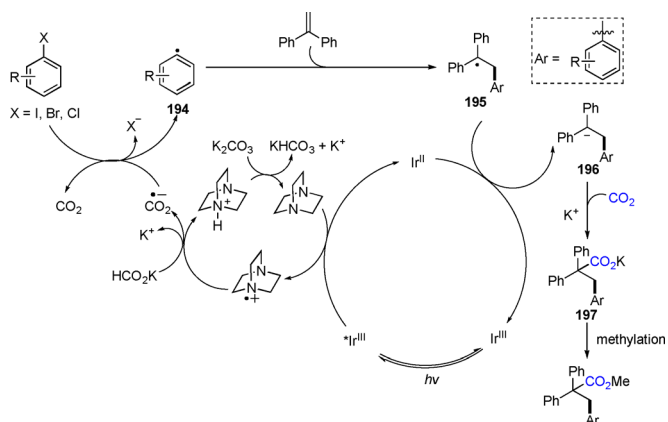
## A) Selected substrate scope of aryl halides and alkyl halides



## B) Selected examples of heterocyclic incorporation

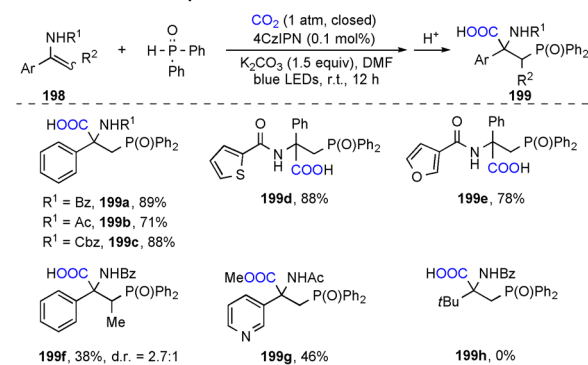


**Scheme 37.** Visible-light-driven reductive carboxylation of styrenes with CO<sub>2</sub> and aryl halides.

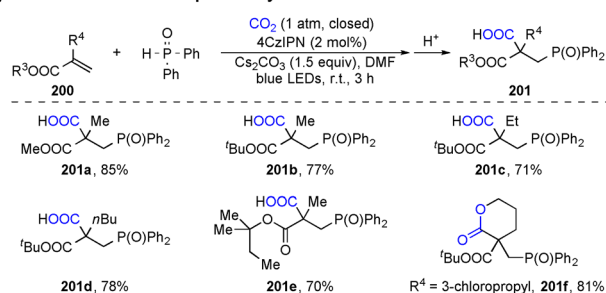


**Scheme 38.** Proposed catalytic cycle for reductive carboxylation of styrenes.

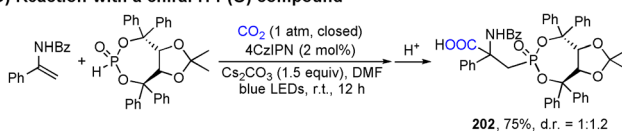
## A) Selected substrate scope of enamides



## B) Selected substrate scope of acrylates



## C) Reaction with a chiral H-P(O) compound

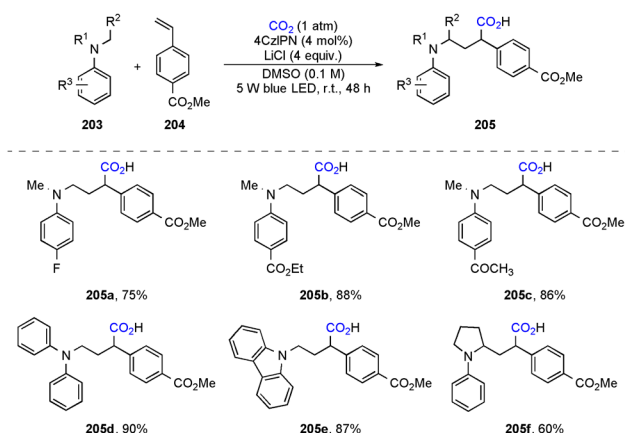


**Scheme 39.** Phosphonocarboxylation of alkenes with carbon dioxide via visible-light promoted photoredox catalysis.

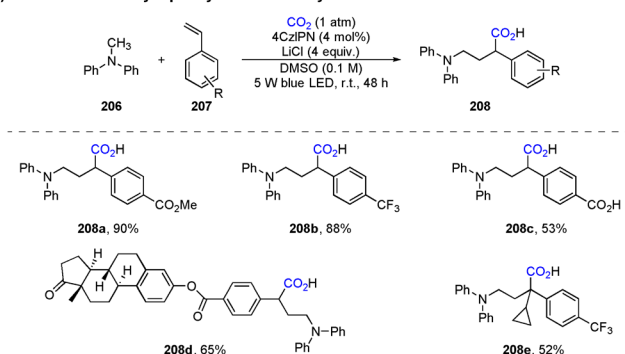
Yu and co-workers expanded the scope of the visible-light-mediated difunctionalization of alkenes to phosphonocarboxylation with enamides and acrylates (Scheme 39).<sup>[63]</sup> A range of aryl enamides were difunctionalized, providing various β-phosphono α-amino acids **199** bearing a quaternary carbon center with moderate to excellent yields (Scheme 39A). However, the hydrophosphinylation product instead of the desired carboxylate product was obtained when an alkyl enamide was used. Phosphonocarboxylation of various acrylates is shown in Scheme 39B, although hydrophosphinylation of electron-deficient alkenes with phosphine oxides and phosphites (H-P(O)) compounds via nucleophilic addition has been well documented. Notably, an enantio-enriched H-P(O) compound derived from a (4*R*,5*R*)-taddol derivative was used for an enantioselective transformation with CO<sub>2</sub>, which resulted in poor diastereoselectivity (Scheme 39C). Preliminary mechanistic studies revealed an α-amino benzylic anionic species as the key intermediate and the involvement of a reductive quenching photoredox catalytic cycle.

More recently, Xi and co-workers reported a visible-light-promoted carboxylation of styrenes using CO<sub>2</sub> and amines catalyzed by photocatalyst 4CzIPN to access γ-amino acids **205** and **208** (Scheme 40).<sup>[64]</sup> Mechanistically, photoexcited 4CzIPN is reduced by aniline **209** via SET to give a radical cation intermediate **210**, which is deprotonated to

## A) Reactions of methyl 4-vinylbenzoate with amines



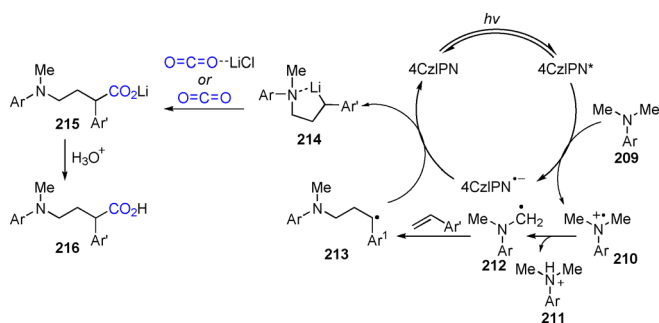
## B) Reactions of methyldiphenylamine with styrenes



**Scheme 40.** Photoredox-catalyzed dicarboxylation of styrenes with amines and CO<sub>2</sub>.

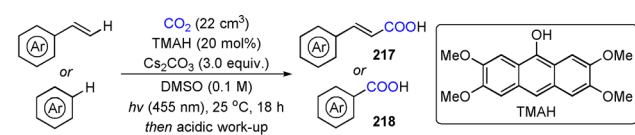
form an  $\alpha$ -amino carbon radical species **212**. A subsequent radical addition of **212** to styrene generates a  $\gamma$ -amino benzylic radical **213**, which is reduced by the reduced 4CzIPN radical anion via a SET to afford a  $\gamma$ -3-amino benzylic carbanion **214**, proposed as a lithium chelated species. A subsequent nucleophilic addition of **214** to CO<sub>2</sub> or LiCl activated CO<sub>2</sub> and protonation provides the desired  $\gamma$ -amino acid (Scheme 41).

More recently, König and co-workers reported a redox-neutral photocatalytic C–H carboxylation of styrenes with CO<sub>2</sub> using 2,3,6,7-tetramethoxyanthracen-9(10H)-one (TMAH) as the photocatalyst under blue light excitation.<sup>[65]</sup> Their protocol provides a direct access to *trans*-cinnamic acid

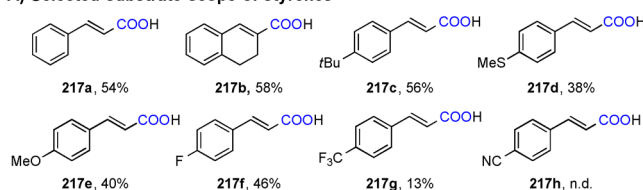


**Scheme 41.** Proposed reaction mechanism for the synthesis of  $\gamma$ -amino acid.

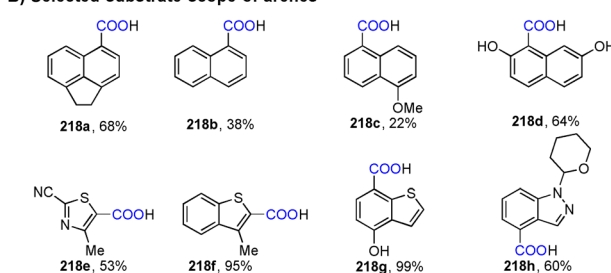
derivatives, in contrast to the existing light-mediated hydrocarboxylation of styrenes (Scheme 42A). The substrates bearing electron-donating groups (**217c–217e**) or weak electron-withdrawing groups (**217f**) were able to give corresponding product in good yield. When stronger electron-withdrawing group was applied (**217g**), a lower yield was observed. Moreover, 4-cyanostyrene (**217h**) was not suitable for this reaction. A possible mechanism has been proposed based on a series of mechanistic investigation, (Scheme 42C). The photocatalyst TMAH is deprotonated by cesium carbonate to form an anionic species TMA<sup>-</sup>, which under visible light irradiation generates a strongly-reducing excited anion \*TMA<sup>-</sup> [ $E(TMA^*/^*TMA^-) = -2.92$  V vs. SCE]. Although a direct reduction of CO<sub>2</sub> by \*TMA<sup>-</sup> is thermodynamically feasible, the luminescence lifetime of \*TMA<sup>-</sup> in the CO<sub>2</sub>-saturated solution of DMSO remained almost unchanged in the Stern–Volmer experiment, which indicates a kinetic barrier preventing the formation of CO<sub>2</sub> radical anion. On the other hand, the luminescence lifetime of \*TMA<sup>-</sup> decreased obviously in the presence of styrene, demonstrating that a SET between \*TMA<sup>-</sup> and styrene initiates the reaction. Then a radical anion **219** traps CO<sub>2</sub> to give a radical carboxylate **220**. Oxidation of **220** by TMA<sup>-</sup> via SET generates



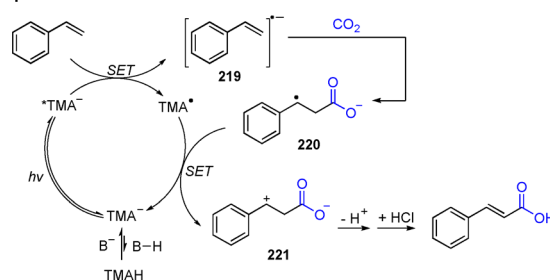
## A) Selected substrate scope of styrenes



## B) Selected substrate scope of arenes



## C) Proposed mechanism



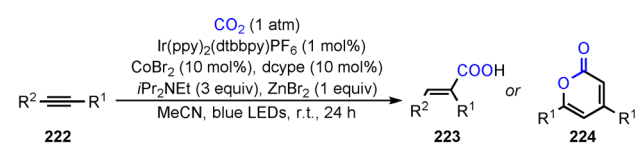
**Scheme 42.** Redox-neutral photocatalytic C(sp<sup>2</sup>)-H carboxylation of styrenes and (hetero)arenes.



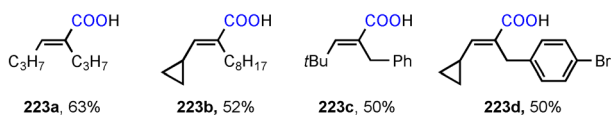
a benzylic cation **221** followed by a deprotonated elimination to give the carboxylate product. According to the proposed mechanism, electron-deficient styrenes lead to reduced yield since electron-withdrawing groups can stabilize the radical anion intermediate and reduce its nucleophilicity to CO<sub>2</sub>. Notably, this protocol can be extended to a series of arenes to achieve directly C(sp<sup>2</sup>)-H carboxylation with CO<sub>2</sub>, including naphthalene derivatives (**218a–218d**) and heteroaromatic compounds (**218e–218h**, Scheme 42 B).

### 3.2.3. Visible-Light-Promoted Carboxylation of Alkynes with Carbon Dioxide

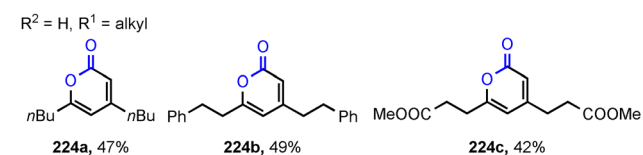
Substituted alkenes are important structural motifs found in pharmaceuticals, agrochemicals and biologically active natural products and are also versatile building blocks in organic synthesis.<sup>[66]</sup> Access of alkenes through the direct functionalization of alkynes represents a straightforward pathway. Although several groups have reported transition-metal-catalyzed alkyne hydrocarboxylation, the molecular scaffolds compatible with these protocols were limited to linear acrylic acids and 2-pyrones.<sup>[67]</sup> Furthermore, stoichiometric amounts of reductants, such as Et<sub>2</sub>Zn, silanes, Mn, or Zn, were required. The first breakthrough that overcame these limitations was reported by Wu, Zhao, and co-workers, who developed the first visible-light-driven hydrocarboxylation and carbocarboxylation of alkynes using CO<sub>2</sub> in a Ir/Co dual catalysis system.<sup>[68]</sup> Both aryl and aliphatic substituted internal alkynes are good candidates for this transformation (Scheme 43). In general, the regioselectivity of this reaction is dependent on the relative steric environment of the unsymmetrical alkyne, where the CO<sub>2</sub> insertion happens adjacent to the less sterically hindered substituent. Notably, it was observed that aryl bromides, which were usually incompatible with metal reductants, can be tolerated in this protocol generating products such as **223d**. Interestingly, 2-pyrones were generated when terminal alkynes were employed, representing a rare case of synthesis of 2-pyrones **224** via



#### Hydrocarboxylation



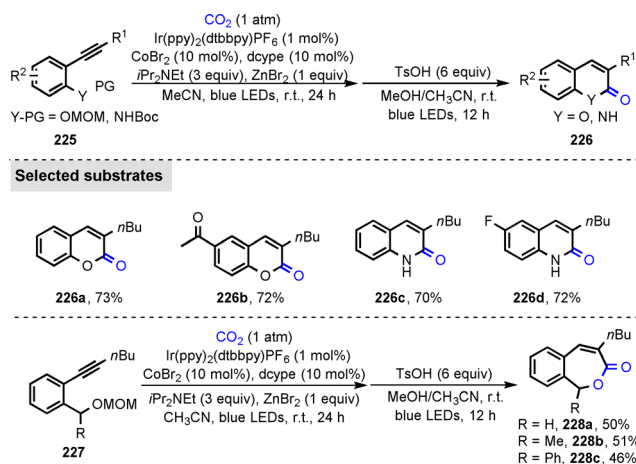
#### [2+2+2] cycloaddition with CO<sub>2</sub>



**Scheme 43.** Visible light driven Co-catalyzed alkyne hydrocarboxylation and [2+2+2] cycloaddition with CO<sub>2</sub>.

intermolecular [2+2+2] cycloaddition between two alkynes and CO<sub>2</sub>.

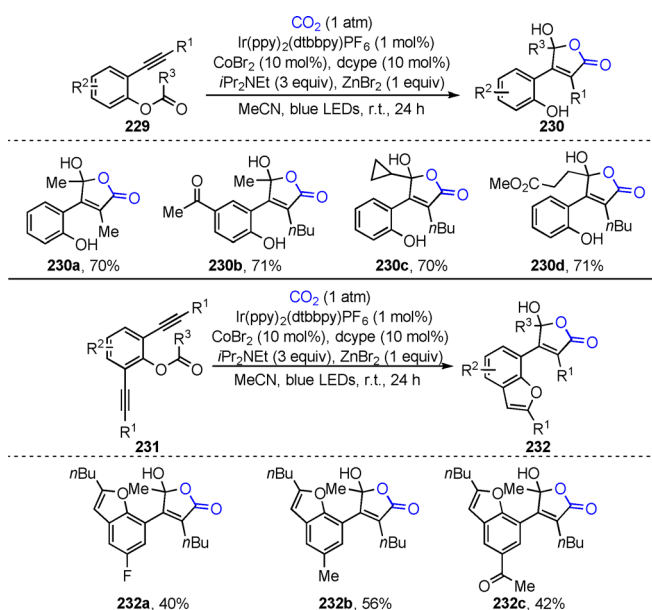
Upon the introduction of an ancillary substituent on the aryl ring, various products, such as coumarins, 2-quinolones and 2-benzoxepinones, could be accessed directly through a one-pot alkyne hydrocarboxylation/alkene isomerization/cyclization sequence (Scheme 44). Here, the Ir photocatalyst



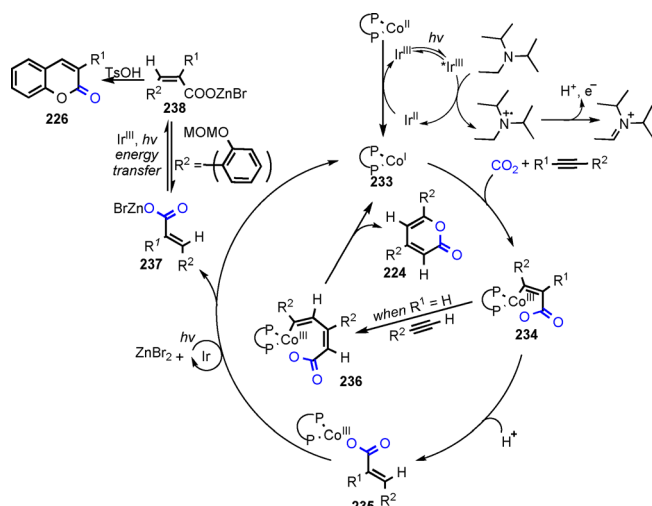
**Scheme 44.** Visible light driven Co-catalyzed one-pot aryl alkyne hydrocarboxylation/alkene isomerization/cyclization reaction. MOM = methoxymethyl acetal; dcype = 1,2-bis(dicyclohexylphosphino)ethane.

plays two roles. First, it promotes the single electron transfer in alkyne hydrocarboxylation and second, energy transfer in the following alkene isomerization. Notably, this method could also generate seven-membered heterocycles **228** by switching phenyl ether substituted alkynes to benzyl ether substituted alkynes, highlighting its utility in accessing heterocycles with different ring sizes. Based on the hypothesis that a five-membered cobaltacycle intermediate derived from the Co species, alkynes and CO<sub>2</sub> might be involved in the process, the authors strategically incorporated an electrophilic substituent in the alkyne substrate to trigger a kinetically favored intramolecular addition of the cobaltacycle intermediate, realizing alkyne difunctionalization. Indeed,  $\gamma$ -hydroxybutenolides **230** and **232** could be obtained using CO<sub>2</sub> with *ortho*-ester substituted aryl alkynes under the photoredox/cobalt dual catalytic conditions (Scheme 45), serving as a novel method to access these interesting structural motifs, which can be found in natural products such as ianthellidone G, manoalide and petrosaspongiolide M, and in pharmaceutically important agents.

Mechanistically, the transformation is initiated by reductive quenching of visible light-excited Ir<sup>III</sup> with iPr<sub>2</sub>NEt to yield a reduced Ir<sup>II</sup> species and an amine radical cation. The Ir<sup>II</sup> species [ $E_{1/2}(\text{Ir}^{\text{III}}/\text{Ir}^{\text{II}}) = -1.51$  V vs. SCE in MeCN] is then oxidized by a Co<sup>II</sup> species ( $E_{1/2} = -0.72$  V vs. SCE in MeCN) to regenerate Ir<sup>III</sup> and yield a Co<sup>I</sup> species **233**. Co<sup>I</sup> **233** couples with CO<sub>2</sub> and alkynes to form the key five-membered Co<sup>III</sup> cobaltacycle intermediate **234** (Scheme 46). Protonolysis of the C–Co<sup>III</sup> bond by cationic amine radicals would yield the carboxylatocobalt intermediate **235**, which may undergo photoreduction to regenerate **233**. ZnBr<sub>2</sub> aids in this process

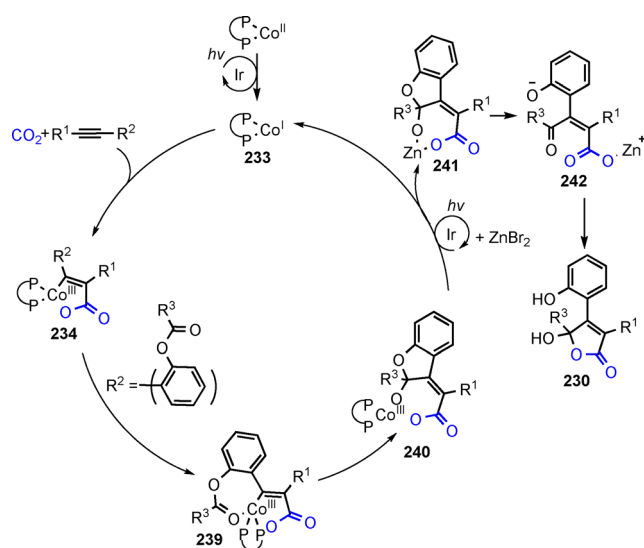


**Scheme 45.** Synthesis of  $\gamma$ -hydroxybutenolides from *ortho*-ester substituted aryl alkynes and  $\text{CO}_2$  driven by light irradiation.



**Scheme 46.** Proposed mechanism of visible light driven Co-catalyzed alkyne hydrocarboxylation and [2+2+2] cycloaddition with  $\text{CO}_2$ .

by transmetalation to furnish a carboxylate **237**. An Ir-mediated triplet-triplet energy transfer process followed by an acid-mediated intramolecular cyclization delivers the desired product **226**. In the case of terminal alkynes, migratory insertion of another alkyne molecule into the five-membered ring **234** would yield a seven-membered cobaltacycle **236**, which then undergoes reductive elimination to yield 2-pyrones **224**.  $\gamma$ -Hydroxybutenolides **230** were obtained in high yields through an unprecedented Co carboxylation/acyl migration cascade process when an *ortho*-ester-substituted aryl alkyne was employed as the alkyne substrate (Scheme 47). The intramolecular addition of the C–Co<sup>III</sup> bond generated in situ to the ester substituent provides carbo-carboxylation intermediate **240** which then undergoes photoreduction and transmetalation to yield the



**Scheme 47.** Proposed mechanism of light mediated  $\gamma$ -hydroxybutenolide synthesis from *ortho*-ester substituted aryl alkynes and  $\text{CO}_2$ .

Zn complex **241**. Complex **241** underwent two rounds of tautomerization to yield  $\gamma$ -hydroxybutenolides **230**.

### 3.2.4. Visible-Light-Promoted Carboxylation of Enamides and Imines with Carbon Dioxide

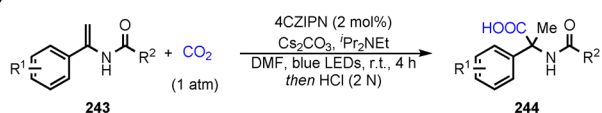
While the utilization of  $\text{CO}_2$  as an abundant and reusable raw material has attracted significant interest, the construction of amino acids utilizing  $\text{CO}_2$  as a C1 source represents one particularly intriguing but challenging transformation. There is an impetus to develop new methods for the catalytic hydrocarboxylation of readily available enamides or imines for this important family of bioactive compounds.

The first catalytic, transition metal-free light-promoted hydro-carboxylation of enamides and imines was pioneered by the Yu group in 2018, who used 1 atm of  $\text{CO}_2$  to generate important  $\alpha,\alpha$ -disubstituted  $\alpha$ -amino acids (Scheme 48).<sup>[69]</sup> Through the generation of  $\alpha$ -amino carbanions achieved by visible-light-driven reduction of enamides, they were able to overcome the inherent nucleophilicity at the  $\beta$ -position of enamides, leading to selective formation of  $\alpha$ -amino acids. A wide range of aryl enamides (Scheme 48A) and aryl imines (Scheme 48B) could be applied using *iPr*<sub>2</sub>NEt as a reductant. Subsequently, the same group realized a visible-light-mediated phosphonocarboxylation of enamides as described in Scheme 39A.

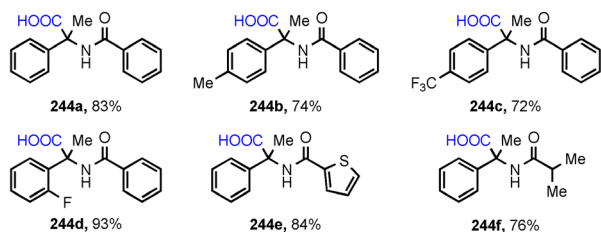
Walsh and co-workers reported a visible light-mediated, Ir(ppy)<sub>2</sub>(bpy)PF<sub>6</sub>-catalyzed hydrocarboxylation of non-protected aryl imines with *N,N*-dicyclohexylmethylamine (Cy<sub>2</sub>NMe) as a sacrificial electron donor for the synthesis of  $\alpha,\alpha$ -disubstituted  $\alpha$ -amino acids (Scheme 49).<sup>[70]</sup> This method has good functional group compatibility, tolerating aryl chlorides (**248d**), aryl(hetero)cycles (**248b**, **248e**) and allyl groups (**248c**) to provide these  $\alpha$ -amino acids with moderate to excellent yields.

The authors proposed that the coordination of an amine radical cation and imines forms a complex **249** which contains

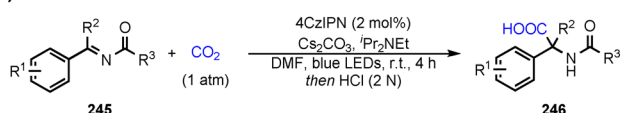
## A) Enamides



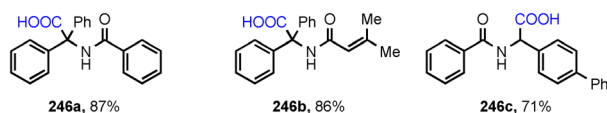
## Selected substrates



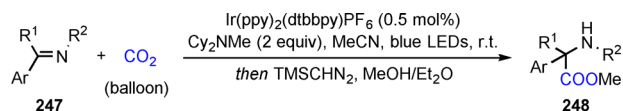
## B) Imines



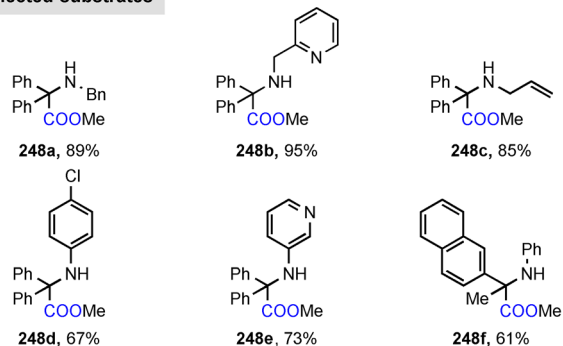
## Selected substrates



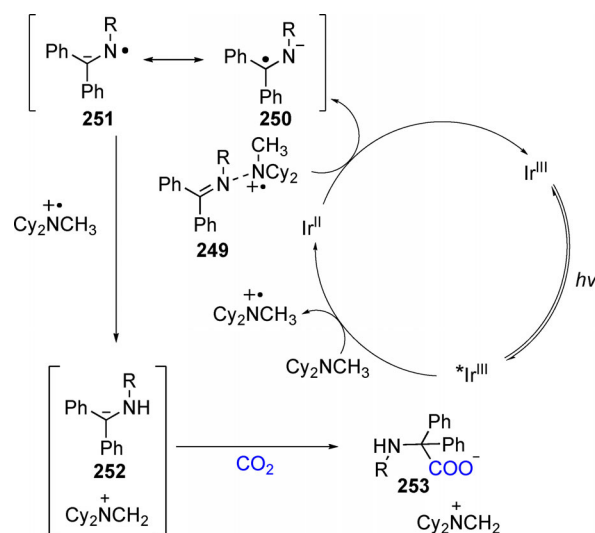
Scheme 48. Hydrocarboxylation of a) enamides and b) imines.



## Selected substrates

Scheme 49. Visible light-mediated catalytic hydrocarboxylation of ketimines using CO<sub>2</sub>.

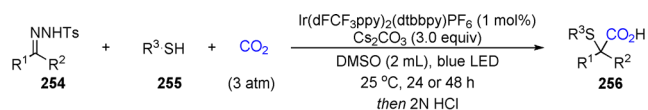
a 2-center-3-electron bond, facilitating the reduction by Ir<sup>II</sup> to form the radical anion intermediate (**250/251**). Ir<sup>III</sup> is regenerated in the process (Scheme 50). The highly reactive *N*-radical **251** is quickly quenched by the amine radical cation via HAT to form the  $\alpha$ -amino carbanion intermediate **252**. Intermediate **252** acts as a strong nucleophile and reacts with CO<sub>2</sub> to give the adduct **253**, which after methylation affords the ester product. A key factor in controlling the reactivity is the resonance form of **251**, which has a greater spin density on the nitrogen (0.37) than on the diaryl substituted carbon (0.18), indicating that diaryl substituted carbon carries more anionic characters.



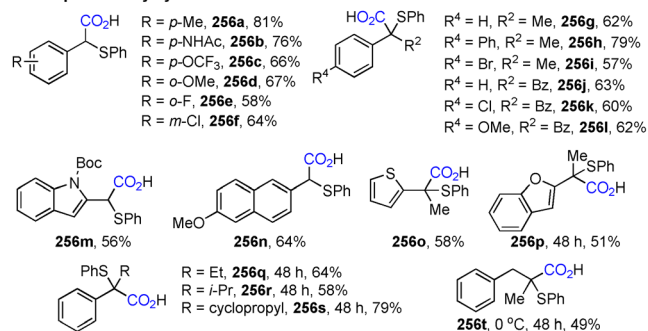
Scheme 50. Proposed mechanism for catalytic hydrocarboxylation of ketimines under light irradiation.

3.2.5. Visible-Light-Promoted Carboxylation of *N*-sulfonylhydrazones

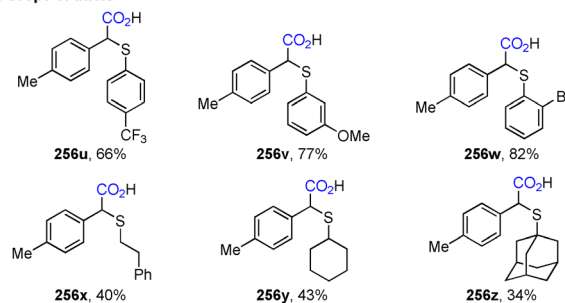
Recently, the König group reported a photo-Wolff-Kishner type thiocarboxylation of *N*-tosylhydrazones assisted by Ir<sup>III</sup>-based photoredox catalysis (Scheme 51).<sup>[71]</sup> A series of aromatic aldehyde-derived *N*-tosylhydrazones (**256a–256f**,



## Selected substrates

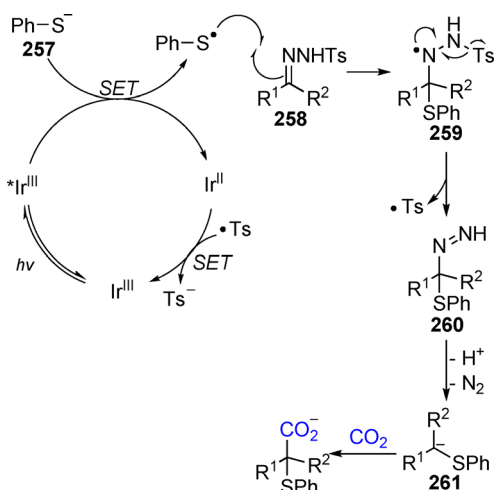
The scope of *N*-tosylhydrazones

## The scope of thiols

Scheme 51. Photo-Wolff-Kishner type thiocarboxylation of *N*-tosylhydrazones.

**256 m–256 n**) and ketone-derived *N*-tosylhydrazones (**256 g–256 l**, **256 o–256 p**) bearing various functional groups proved to be effective substrates. Increasing the steric hindrance at the  $\alpha$ -position of the *N*-tosylhydrazones failed to decrease the product yield (**256 q–256 s**). Notably, the thiocarboxylation of a substrate **256 t** derived from an aliphatic ketone was also achieved at a low temperature (0 °C). The scope of thiols was also evaluated. Thiophenols with electron-donating (**256 v**) or electron-withdrawing groups (**256 u**, **256 w**) were well tolerated and aliphatic thiols (**256 x–256 z**) were also able to generate the desired products in moderate yields.

The authors proposed a plausible mechanism (Scheme 52) based on a series of spectroscopic investigations and control experiments. This reaction is initiated by a SET between thiophenolate and the excited photoredox catalyst. *N*-tosylhydrazone is added by the resulting sulfur radical to generate the aminyl radical species **259**. Then, a functionalized diazene intermediate **260** is formed by the fragmentation of this radical species **259**, and an arenosulfonyl radical is produced simultaneously. Intermediate **260** subsequently undergoes a Wolff–Kishner type nitrogen extrusion process to give a  $\alpha$ -sulfur carbanion **261** which attacks CO<sub>2</sub> to produce the thiocarboxylated product. The photoredox catalytic cycle is turned over by another SET between the arenosulfonyl radical and Ir<sup>II</sup>.

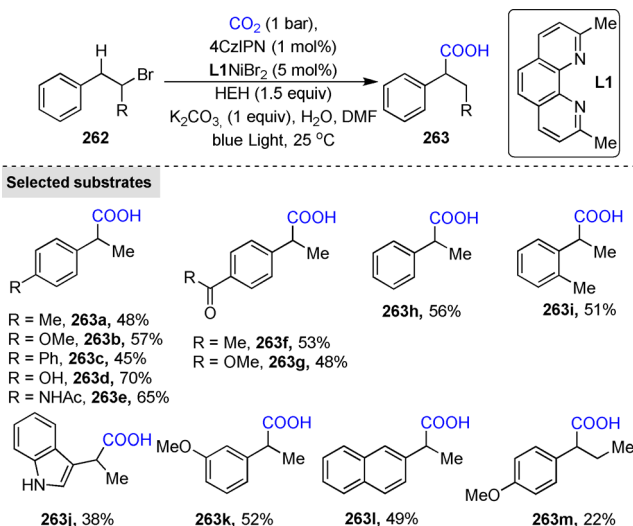


**Scheme 52.** Proposed mechanism of photo-Wolff–Kishner type thiocarboxylation.

### 3.2.6. Visible-Light-Promoted Carboxylation of C(sp<sup>3</sup>)–H bonds

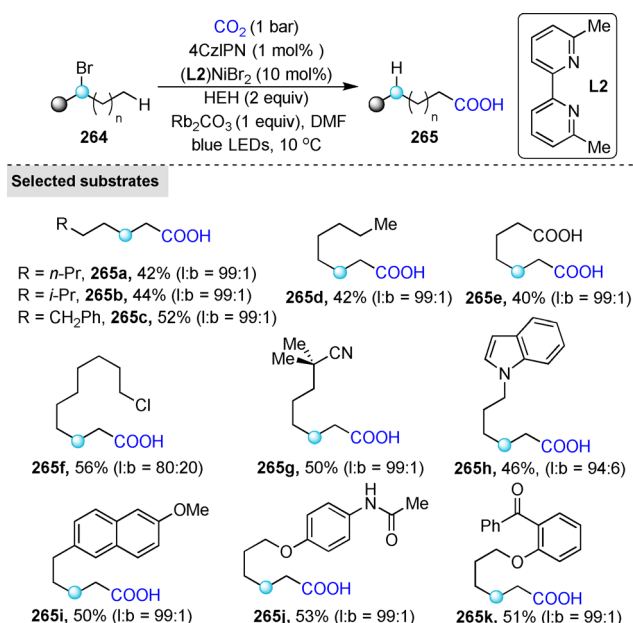
There has been much development in the activation of C(sp<sup>3</sup>)–H bond, but the direct carboxylation of C(sp<sup>3</sup>)–H bonds remains limited to acidic C(sp<sup>3</sup>)–H bonds, or requires harsh conditions and UV-light.<sup>[72]</sup> In 2019, Martin and König collaborated to demonstrate a selective C(sp<sup>3</sup>)–H carboxylation reaction catalyzed by the merger of photoredox and Ni catalysis.<sup>[73]</sup> The selectivity of the C–H bond carboxylation was controlled through an alkyl bromide-induced Ni-chain walking process. The choice of ligand had a major impact on the selectivity. Subtle changes in substituents on carbons adjacent to the nitrogen atoms in the ligand can lead to

a marked decrease in reactivity, and ligand **L1** appeared to be the optimal ligand for both reactivity and selectivity. The use of desiccants led to lower yields, suggesting that water played a significant role in the reaction. The carboxylation at benzylic sp<sup>3</sup> C–H bond showed excellent selectivity and functional group tolerance, although products (**263**) were obtained in moderate yields (Scheme 53).



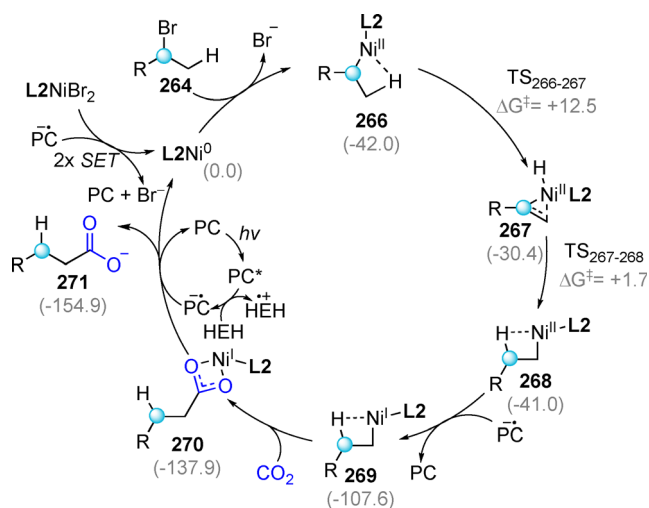
**Scheme 53.** Substrate scope of benzylic C(sp<sup>3</sup>)–H carboxylation.

In addition to benzylic C(sp<sup>3</sup>)–H bonds, the reaction is also compatible with non-activated alkanes, and the highest efficiency was achieved by using **L2** (Scheme 54). The reaction was found to tolerate a variety of functional groups, such as esters, nitriles (**265 g**), ketones (**265 k**), alkyl chlorides (**265 f**), amides (**265 j**) and indoles (**265 h**). Most



**Scheme 54.** Carboxylation of C(sp<sup>3</sup>)–H bonds on alkanes.



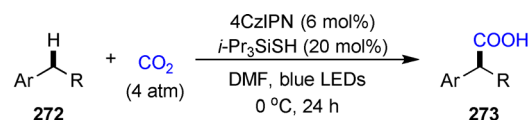


**Scheme 55.** Proposed C(sp<sup>3</sup>)-H carboxylation mechanism and calculated Gibbs free energy of intermediates (kcal mol<sup>-1</sup>).

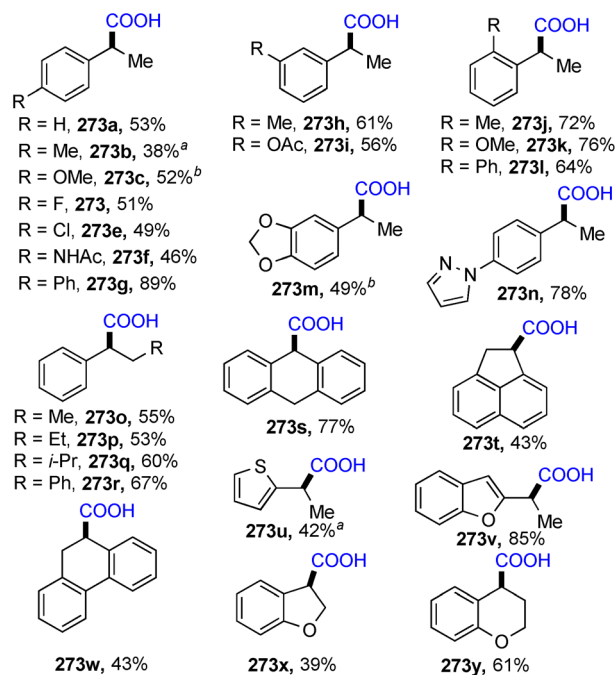
substrates showed high selectivity for the desired linear products over the branched products.

Through combined computational and experimental studies, the authors proposed a plausible mechanism that begins with the reduction of Ni<sup>II</sup> to Ni<sup>0</sup> (Scheme 55). Ni<sup>0</sup> then undergoes an oxidative addition to the alkyl bromide to produce an alkyl-Ni<sup>II</sup> complex **266**. DFT calculations suggested that complexes **266–268** have similar energies and exist in rapid equilibrium via facile β-H elimination from cationic Ni<sup>II</sup> intermediates. It was also suggested by DFT calculations that CO<sub>2</sub> insertion was less favorable for the Ni<sup>II</sup> complex, thus supporting CO<sub>2</sub> insertion through a Ni<sup>I</sup> complex. Insertion of CO<sub>2</sub> into the Ni-C bond of Ni<sup>I</sup> species **269** yields a Ni-carboxylate **270**. Ni-carboxylate **270** then undergoes a SET to produce the carboxylate **271** and regenerate Ni<sup>0</sup>.

Another breakthrough in the field of visible light-mediated direct carboxylation of sp<sup>3</sup> C-H bonds was achieved by König and co-workers when they presented a metal-free approach to the carboxylation of the benzylic C(sp<sup>3</sup>)-H bonds through an indirect HAT process, mediated by a triisopropylsilane thiol HAT catalyst.<sup>[74]</sup> The reaction shows a broad substrate scope of benzylic type compounds, including electron-withdrawing and electron-donating substituents, as well as cyclic and heterocyclic compounds (Scheme 56). Notably, in the case where there is more than one benzylic C-H site in the substrate, monocarboxylated acids (**273s**, **273t**, **273w**) are formed exclusively. The applicability and efficiency of this protocol was demonstrated through the synthesis of several drug molecules containing the structural motif of 2-phenylpropionic acid, such as fenopropfen (**274**), flurbipropfen (**275**), naproxen (**276**) and ibuprofen (**277**) (Scheme 57). In the case of ibuprofen, where two sets of benzylic protons are present, a selective formation of ibuprofen **277** over the alternative product **278** was observed. The high chemoselectivity can be presumably attributed to the steric environment adjacent to the benzylic protons, where the carboxylation leading to ibuprofen was less sterically hindered and thus favored.

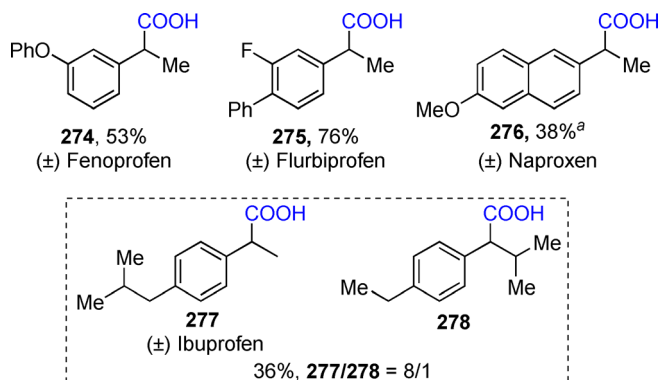


#### Selected substrates



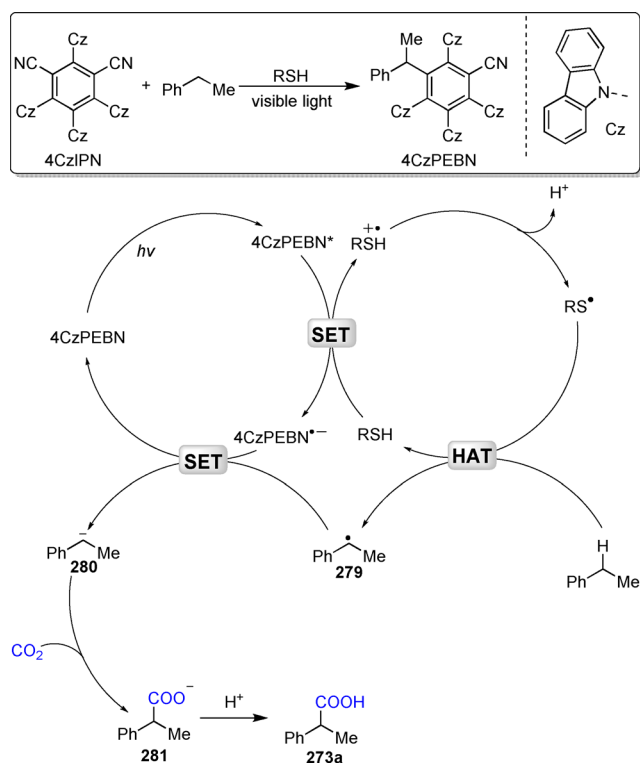
**Scheme 56.** Substrate scope of benzylic C(sp<sup>3</sup>)-H carboxylation.

<sup>a</sup>4CzIPN was replaced by 3DPAFIPN. <sup>b</sup>4CzIPN was replaced by 3DPA2FBN. 3DPAFIPN: 2,4,6-tris(diphenylamino)-5-fluoroisophthalonitrile. 3DPA2FBN: 2,4,6-tris(diphenylamino)-3,5-difluorobenzonitrile.



**Scheme 57.** Synthesis of pharmaceutical compounds containing 2-phenylpropionic acid motif. <sup>a</sup>4CzIPN was replaced by 3DPAFIPN. <sup>b</sup>4CzIPN was replaced by 3DPA2FBN.

During the mechanistic investigation of the photocatalytic decarboxylation, it was observed that a cyano (CN) group on 4CzIPN was replaced by an ethylbenzene moiety. This formed 2,3,4,6-tetra(9H-carbazol-9-yl)-5-(1-phenylethyl)benzonitrile (4CzPEBN), which was proposed as the active photocatalyst to catalyze the reaction. 4CzPEBN is excited by light [ $E_{1/2}(\text{PC}^+/\text{PC}^*) = +1.19$  V vs. SCE], and then the thiol HAT catalyst ( $E_{1/2}^{\text{ox}} = +0.28$  V vs. SCE)<sup>[75]</sup> is oxidized, yielding a reduced 4CzPEBN<sup>-</sup> (Scheme 58). The oxidized thiol



**Scheme 58.** Proposed mechanism for benzylic C(sp<sup>3</sup>)-H carboxylation.

catalyst then loses a proton to yield a thiol radical ( $BDE_{S-H} = 88.2 \text{ kcal mol}^{-1}$ ). The thiol radical abstracts a hydrogen from the benzylic C-H bonds ( $BDE_{C-H} = 85.4 \text{ kcal mol}^{-1}$ )<sup>[75]</sup> to yield a benzylic radical **279**, regenerating the thiol catalyst. The benzylic radical ( $E_{1/2}^{\text{red}} = -1.60 \text{ V vs. SCE}$  for the phenylethyl radical)<sup>[76]</sup> is then reduced by 4CzPEBN<sup>-•</sup> [ $E_{1/2}(\text{PC}/\text{PC}^{\bullet-}) = -1.69 \text{ V vs. SCE}$ ] to form a carbanion **280** and regenerate the photocatalyst. The anion **280** is then captured by CO<sub>2</sub>, and is protonated to yield the carboxylic acid **273a**.

The recent development of light-driven carboxylation utilizing CO<sub>2</sub> as a C1 source to access value-added chemicals has been briefly summarized in this section. These works represent novel activation modes complementary to existing transition-metal catalyst approaches and have inspired new perspectives for utilizing CO<sub>2</sub> in carboxylation, which can produce useful compounds for the agrochemical and pharmaceutical industries. Considering the rapid development in photocatalysis, we foresee that photo-mediated carboxylation

using CO<sub>2</sub> will continue to progress rapidly to achieve challenging and previously inaccessible transformations, enabling greener and more sustainable protocols for fine chemical synthesis using CO<sub>2</sub>.

#### 4. Gaseous Alkenes and Alkynes

Gaseous alkenes and alkynes, such as ethylene, propene, 1,3-butadiene and acetylene, are important industrial feedstock chemicals for the synthesis of value-added chemicals. However, most light-promoted reactions involving such unsaturated gaseous compounds are limited to photo-cyclo-additions.<sup>[77]</sup> In 2017, the Wu group developed a “stop-flow” micro-tubing (SFMT) reactor enabling efficient, safe and convenient screening of photo-mediated transformations involving the aforementioned gases (Figure 2).<sup>[78]</sup> The SFMT reactor platform is a design adapted from continuous flow systems with the addition of batch elements. Instead of allowing the reaction mixture to flow through the tubing continuously, the SFMT platform allows the flow to be stopped at will. The platform differs from earlier approaches in that the SFMT is based on a “switch in-and-out” approach using shut-off valves on each end of the micro-tubing reactor. This means that the SFMT system can be used as an independent module, in which the reactor can be filled at a pre-determined pressure maintained by a back-pressure regulator (BPR) with both valves closed and disconnected from the system. Multiple isolated reactors can be placed in parallel under the determined reaction conditions until the desired reaction time has been achieved. Thus, each of the sealed micro-tubing reactors behaves like a high-pressure reactor. The SFMT reactor may possess a poorer mixing efficiency compared to stirring in batch reactors, or circular flow patterns from Taylor flow, but the excellent gas-liquid interfacial contact in the SMFT reactor can still result in good reaction efficiency. An added advantage is that, compared to continuous flow techniques, reaction screening with SFMT reactors can save time by parallel screening. The residence time is not limited by the reactor size and can be held for as long as necessary.

SFMT reactors provide a simple and effective platform for photosynthesis using gaseous reagents, especially at high pressures. Wu and co-workers were able to achieve the photocatalytic vinylation of fluorinated aryl bromides **282** using acetylene gas in moderate to high yields assisted by the

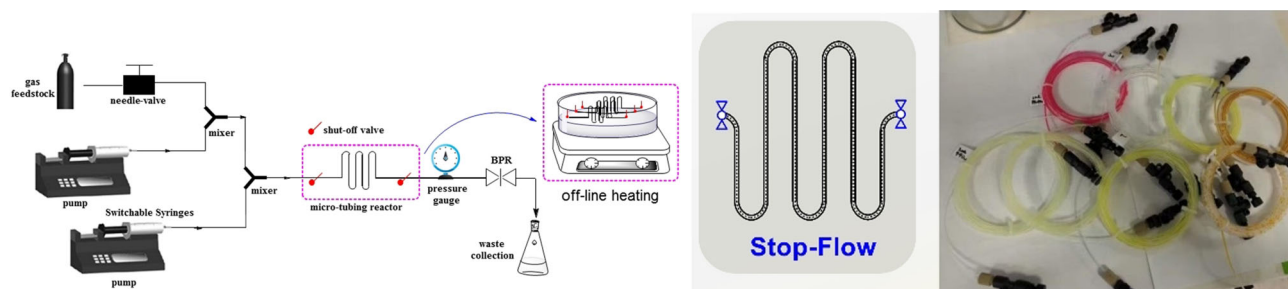
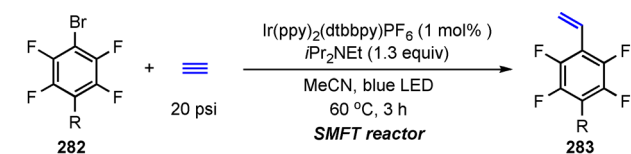


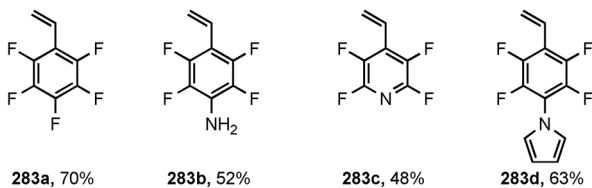
**Figure 2.** The development of “stop-flow” micro-tubing reactors.







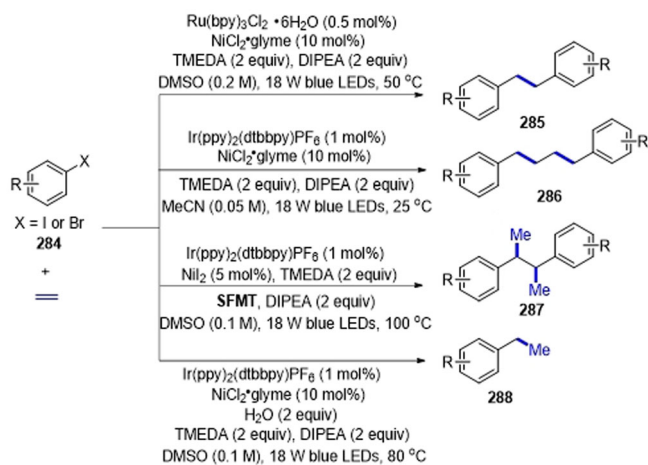
## Selected substrates



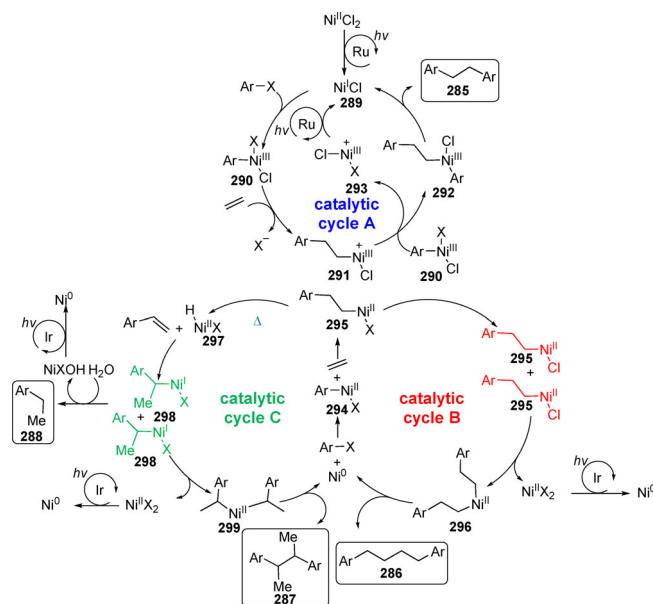
**Scheme 59.** Vinylation of fluorinated aryl bromides using acetylene gas.

SFMT reactors (Scheme 59). In stark contrast, only trace amounts (<5%) of vinylation products were detected in conventional batch reactors. The gases acetylene escaped the reaction solution at 60 °C in conventional batch reactors, while the SFMT reactor can keep the gas within the reaction solution even at high temperatures.

Wu and co-workers developed a divergent synthesis of 1,2-diarylethanes, 1,4-diarylbutanes, 2,3-diarylbutanes, and ethyl-arenes from a common aryl halide and ethylene through the synergistic combination of photoredox and Ni catalysis (Scheme 60).<sup>[79]</sup> By varying the photocatalysts, nickel catalysts, reaction temperature, and ethylene pressure, various products such as reductive Heck products **288**, one or two-ethylene insertion linear products **285** and **286**, and two-ethylene insertion branched products **287** could be obtained in good yields and high selectivity. This is the first report of divergent synthesis achieved by different catalytic pathways accessed through modulating the oxidation state of organometallic catalysts by the use of photoredox catalysts. Notably, the SFMT reactor was employed to keep ethylene in the reaction solution at high temperature and high pressure to deliver the two-ethylene insertion branched products **287**.



**Scheme 60.** Light promoted Ni-catalyzed divergent transformations of ethylene.



**Scheme 61.** Plausible mechanisms for divergent synthesis using ethylene.

The proposed catalytic cycle (Scheme 61, catalytic cycle **A**) for the synthesis of 1,2-diarylethane begins with formation of Ru(bpy)<sub>3</sub>Cl<sub>2</sub>-promoted Ni<sup>I</sup>. Subsequent oxidative addition of aryl halides to the Ni<sup>I</sup> intermediate **289** forms an aryl-Ni<sup>III</sup> species **290**. Migratory insertion of ethylene into aryl-Ni<sup>III</sup> followed by aryl transfer by a transmetalation between **291** and the aryl-Ni<sup>III</sup> species **290** forms an aryl alkyl Ni<sup>III</sup> species **292**. Then a rapid reductive elimination would yield product **285** and regenerate the active Ni<sup>I</sup> catalyst **289**. The cationic Ni<sup>III</sup> species **293** generated during the transmetalation process would be reduced by a Ru-based photoredox cycle to regenerate Ni<sup>I</sup> **289**. For the synthesis of 1,4-diarylbutanes **286** (catalytic cycle **B**), the catalytic cycle starts with the oxidative addition of aryl halides to Ni<sup>0</sup> reduced by Ir-based photoredox cycle to form the Ni<sup>II</sup> species **294**. Ethylene migratory insertion into **294** leads to the formation of alkyl Ni<sup>II</sup> complex **295**. Transmetalation between two molecules of complex **295** followed by reductive elimination produces **296** and Ni<sup>0</sup>. For the catalytic generation of 2,3-diarylbutanes **297** (catalytic cycle **C**), the alkyl Ni<sup>II</sup> complex **295** undergoes a β-hydride elimination triggered by high temperature to yield a Ni hydride species **297**. Insertion of **297** into styrene forms a benzyl Ni intermediate **298**. Subsequent transmetalation between two molecules of **298** followed by reductive elimination affords **287** and regenerates Ni<sup>0</sup>. The reductive Heck-type product **288** could be obtained by quenching the intermediate **298** with water.

## 5. Gaseous Alkanes

The use of gaseous alkanes as inexpensive feedstocks in synthetic transformations is very attractive from an economic standpoint. However, it is often challenging to activate these gaseous alkanes with their strong C(sp<sup>3</sup>)-H bonds, poor

solubility in most solvents and high ionization energies. Furthermore, conventional methods to activate such inert C–H bonds suffer from the lack of chemoselectivity as harsh conditions are often needed,<sup>[80]</sup> and could also lead to functionalization of solvents or over-functionalization of products. To overcome the limitations, elegant transition-metal-catalyzed activation of gaseous alkanes has been reported in the past decades.<sup>[81]</sup> More recently, photoredox catalysis as a new activation mode has been realized. This technology avoids the need for high reaction temperature and directing groups required for the transition-metal-catalyzed C(sp<sup>3</sup>)–H activation.<sup>[82]</sup>

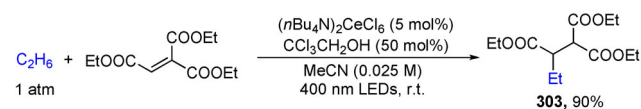
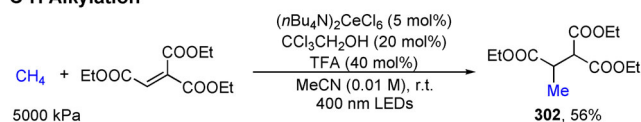
In 2018, Zuo and co-workers developed a selective, photoredox-promoted functionalization of gaseous alkanes process through a synergistic merger of ligand-to-metal charge transfer (LMCT) and HAT catalysis.<sup>[83]</sup> By utilizing inexpensive cerium salts and alcohols as catalysts, the amination of gaseous alkanes (Scheme 62), and the alkylation and arylation of methane and ethane were realized (Scheme 63). Notably, the amination of methane (5000 kPa) and ethane (101 kPa) achieved high turnover numbers of 2900 and 9700 respectively. To demonstrate the robustness of this method, the large-scale application of the reaction was investigated using continuous flow micro-tubing reactors. Remarkably, at a pressure of 1500 kPa for ethane and a flow rate of 0.75 mL min<sup>-1</sup> for the liquid solution stream, the amination product was obtained in 90% yield with a residence time of only 6 min. This translates to a production throughput of 2 mmol h<sup>-1</sup>. On the other hand, the amination of methane only afforded 15% yield due to the pressure limit of commercial flow reactors (1800 kPa). The yield can be improved to 29% with a high-pressure batch reactor (5000 kPa). In addition, methylation and ethylation of electron-deficient alkenes and arylation of methane and ethane were also achieved with moderate to high efficiency (Scheme 63).

The authors proposed that simple alcohols and a Ce<sup>IV</sup> salt would react in situ to generate a Ce<sup>IV</sup>-alkoxy complex which would undergo photo-induced LMCT to generate a high

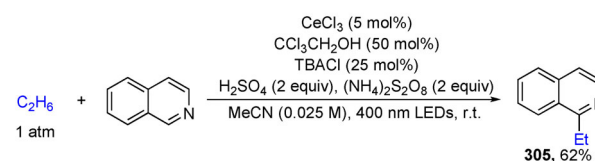
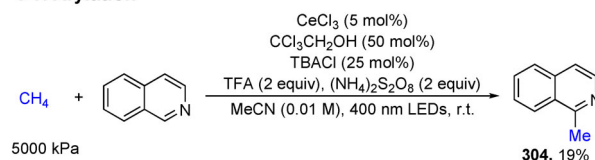
Alkane	Ce catalyst	n	Alcohol	Time (h)	Yield	TON
R = H Methane (5000 kPa)	Ce(OTf) <sub>4</sub>	0.01	CCl <sub>3</sub> CH <sub>2</sub> OH	18	29%	2900
R = Me Ethane (101 kPa)	CeCl <sub>3</sub>	0.01	CCl <sub>3</sub> CH <sub>2</sub> OH	4	97%	9700
R = Et Propane (101 kPa)	CeCl <sub>3</sub>	0.5	CCl <sub>3</sub> CH <sub>2</sub> OH	9	70% (1:1 r.r.)	140
R = Pr Butane (101 kPa)	CeCl <sub>3</sub>	0.5	CCl <sub>3</sub> CH <sub>2</sub> OH	6	76% (1:1.7 r.r.)	152

**Scheme 62.** Cerium-catalyzed amination of gaseous alkanes.

### C-H Alkylation



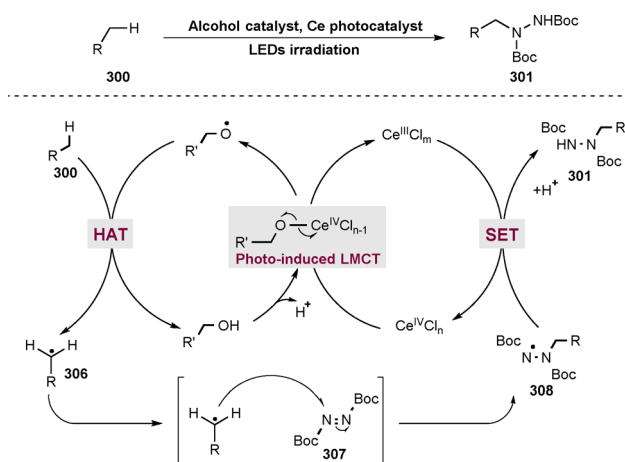
### C-H Arylation



**Scheme 63.** Photocatalytic C–H alkylation and arylation of methane and ethane.

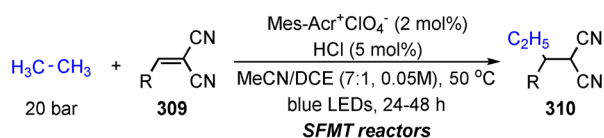
energy electrophilic alkoxy radical and a reduced Ce<sup>III</sup> species (Scheme 64). The alkoxy radical would then abstract a hydrogen atom from the alkane, generating an alkyl radical **306**, which readily couples with di-*tert*-butyl azodicarboxylate (DBAD, **307**) to form a new C–N bond and an *N*-centered radical **308**. This radical would undergo single-electron reduction by the reduced cerium catalyst to regenerate Ce<sup>IV</sup> and also deliver the anionic form of the desired product. The desired product is obtained by final protonation.

The Wu group has reported C–H alkylation and allylation reactions using hydrochloric acid (BDE = 103 kcal mol<sup>-1</sup>) as the HAT catalyst precursor together with Mes-Acr<sup>+</sup> photocatalyst assisted by SFMT reactors (Scheme 65).<sup>[84]</sup> The reported reactions are irreproducible or even inaccessible in conventional batch reactors. Synthetically challenging ethane

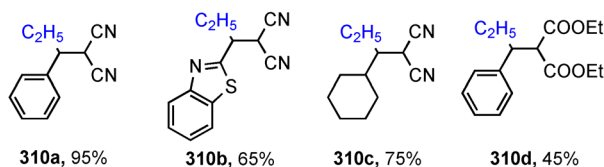


**Scheme 64.** Proposed mechanism for the Ce-catalyzed functionalization of gaseous alkanes under visible-light irradiation.





## Selected substrates

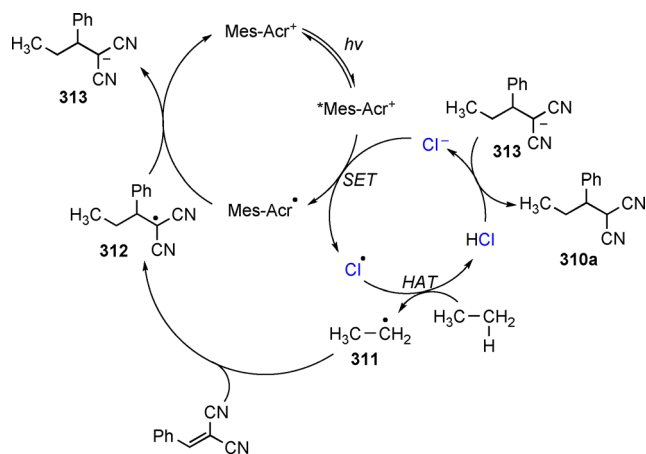


Scheme 65. Functionalization of gaseous ethane.

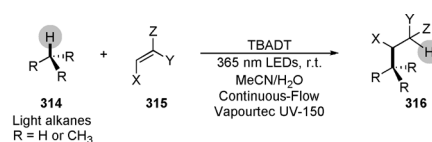
alkylation (Scheme 65) was achieved with strong Michael acceptors, giving alkylated products with moderate to good yields and good functional group tolerance. However, reactions with other alkenes bearing unsaturated ketones or esters were sluggish, presumably due to the fact that the radical adducts formed were not sufficiently strong oxidizing agents to turn over the photoredox catalytic cycle. Gram-scale synthesis using a 27.2 mL tubing reactor was achieved. This example showcased the SFMT reactor for efficient photo synthesis using gas at high pressures and temperatures. It is worth noting that this reaction is probably not suitable for continuous-flow synthesis, as it requires more than 24 h to go to completion.

In the proposed mechanism, the excited state of Mes-Acr<sup>+</sup> could readily oxidize the chloride anion to a chlorine radical, which subsequently abstracts a hydrogen atom from the C(sp<sup>3</sup>)-H partner (ethane) to produce an ethyl radical **311**. Nucleophilic addition of radical **311** to benzylidenemalononitrile would lead to radical adduct **312** which is then reduced by Mes-Acr radical to produce anion **313**, which after protonation yields the ethylation product.

More recently, Noël and co-workers reported a C(sp<sup>3</sup>)-H functionalization of methane, ethane, propane, and isobutane in continuous-flow reactors under 365 nm LED irradiation using decatungstate as the photocatalyst (Scheme 67).<sup>[85]</sup>



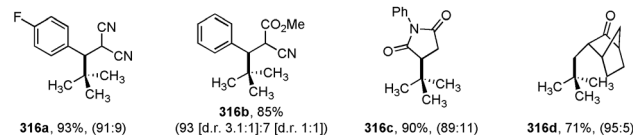
Scheme 66. Proposed mechanism for chlorine-based photo activation of ethane.



## Selected substrates

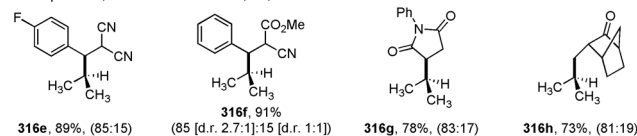
## Light alkane = isobutane

Conditions = TBADT (1.0 mol%), MeCN/H<sub>2</sub>O (7:1), 10 bar pressure, 60 W of 365 nm LEDs, r.t., 4 h



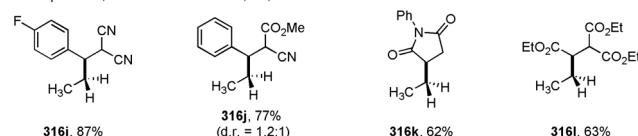
## Light alkane = propane

Conditions = TBADT (1.0 mol%), MeCN/H<sub>2</sub>O (7:1), 10 bar pressure, 60 W of 365 nm LEDs, r.t., 4 h



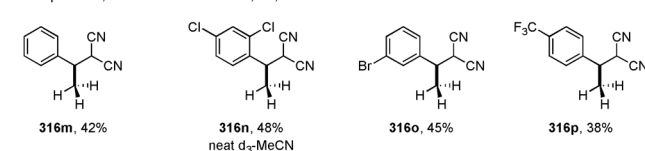
## Light alkane = ethane

Conditions = TBADT (2.0 mol%), MeCN/H<sub>2</sub>O (7:1), 25 bar pressure, 60 W of 365 nm LEDs, r.t., 8 h



## Light alkane = methane

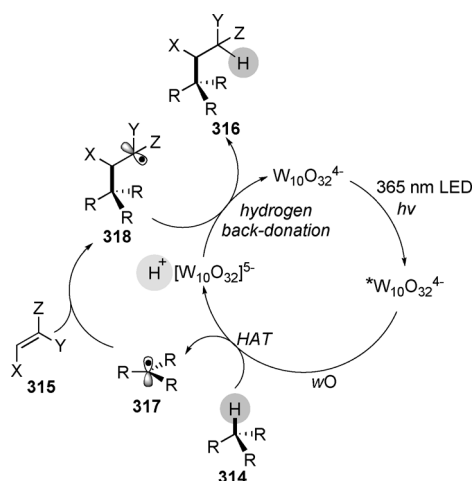
Conditions = TBADT (5.0 mol%), d<sub>3</sub>-MeCN/H<sub>2</sub>O (7:1), 45 bar pressure, 150 W of 365 nm LEDs, r.t., 6 h

Scheme 67. Scope of the decatungstate catalyzed C(sp<sup>3</sup>)-H functionalizations of light hydrocarbons (the ratio in parenthesis reflects the *t*Bu:*i*Bu or *i*Pr:*n*Pr ratio, respectively).

Through the use of a photo hydrogen atom transfer catalyst TBADT in flow, they were able to avoid the use of harsh reaction conditions and obtain hydroalkylated adducts at room temperature in good isolated yields and high selectivity. Significantly, the utilization of flow chemistry provided key advantages over conventional batch reactions that facilitated the successful execution of this transformation. Homogenous irradiation of an entire reaction mixture can be achieved in microflow reactors and allows for efficient generation of alkyl radicals. The low solubility of these gaseous alkanes in organic solvents hampered the development of reactions in batch conditions. Here, the back-pressure regulators in flow allowed high pressure reaction conditions and can force the gaseous alkanes to dissolve in the organic solvents, allowing efficient mix of reagents. Moreover, high pressure reactions in flow are safe and scalable. The authors demonstrated that isobutane (**316a–316d**), propane (**316e–316h**) and ethane (**316i–316l**) can be efficiently functionalized by a variety of activated olefins including benzylidene-malononitriles, methyl *trans*- $\alpha$ -cyanocinnamate, triethyl ethylene-tricarboxylate, *N*-phenylmaleimide and 3-methylene-2-norbornanone with high selectivity. Interestingly, high endo selectivity was observed in the formation of **316d** and **316h**, consistent with a hydrogen back-

donation from the less hindered side of the norbornane moiety. The reaction with methane shows narrower scope and forced conditions are required. Solvent functionalization was observed but could be circumvented by using deuterated acetonitrile.

A tentative mechanism was proposed (Scheme 68). Photoexcitation of decatungstate produces a singlet excited state of decatungstate, which rapidly relaxes to the actual reactive state  $wO$ . A subsequent hydrogen atom transfer from gaseous alkane to  $wO$  forms the carbon-centered radical species **317**. A radical addition of **317** to olefin **315** yields the adduct **318**, which abstracts a hydrogen atom from  $H^+[W_{10}O_{32}]^{5-}$  to form the product **316**.



**Scheme 68.** Proposed mechanism of the decatungstate catalyzed C(sp<sup>3</sup>)-H functionalizations of light hydrocarbons.

## 7. Summary and Outlook

This review has summarized the use of small gas molecules, including carbon monoxide, carbon dioxide, gaseous alkenes, alkynes and alkanes, as feedstocks in the synthesis of fine chemicals under light-irradiation. These gaseous reagents are abundant, inexpensive and readily available carbon-based feedstocks, and are therefore ideal feedstocks in organic synthesis. However, their utilization in synthesis of fine chemicals has been hampered by the difficulty in their handling and is mainly limited to transition-metal catalysis. Their utilization in photochemistry has recently witnessed a remarkable increase of attention in academia. We attribute this to two important reasons. The first reason is the emergence of photo-organic synthesis, which provides various novel activation modes to allow access to previously inaccessible transformations. The second reason is the advances of engineered reaction equipment for simple, convenient, and efficient usage of these gaseous reagents under light-irradiation.

The merits of continuous-flow reactors, including the improved light penetration, the excellent surface to volume ratio, significantly enhanced safety, and easy scaling up, offer a great degree of operational flexibility in the handling of gaseous reagents. The development of stop-flow micro-tubing

(SFMT) reactors which combines the advantages of both batch reactors and flow reactors, provides an excellent platform for light-promoted reaction screening using gaseous reagents, especially at high temperatures and pressures.

Carbon monoxide has been used in UV light-promoted reactions since the 1930s. UV light was used to homolytically cleave chemical bonds to generate radicals which were trapped by CO to form an acyl radical, a key intermediate in carbonylation reactions. Recent development in visible-light-promoted carbonylation reactions involved the use of inexpensive organic dyes, such as fluorescein, eosin Y and 4CzIPN. Photosensitizers based on iridium and ruthenium have also demonstrated excellent catalytic activities. While the carbonylation reactions have demonstrated a sustainable and efficient strategy for construction of a wide range of carbonylated products, the high pressure required for the reactions continues to limit the applicability of the strategy. Recent development of transition-metal catalysis assisted by light activation provides a promising direction for incorporation of CO into complex molecules under mild conditions.

Transition-metal catalysis was widely used to overcome the thermodynamic stability and kinetic inertness of carbon dioxide. Photoredox catalytic systems recently have proven to be more environmentally friendly as they can bypass the need for harsh conditions or stoichiometric amounts of metallic reagents. The methods presented in this review are novel activation modes and are complementary to existing approaches. However, there is an absence of stereoselective transformations for the synthesis of enantioenriched acids and derivatives. Future efforts may be aimed at enantioselective transformations with CO<sub>2</sub>. A promising strategy is to merge photoredox catalysis with transition-metal catalysts equipped with chiral ligands.

Gaseous alkenes and alkynes are important industrial feedstocks in the synthesis of value-added chemicals. The stop-flow micro-tubing reactor is developed to enable more efficient, safe and convenient screening of photo-mediated transformations using these flammable gases. The gases reagents can be sealed in the reaction solutions even at high temperature under photo-irradiation to achieve high efficiency. However, the lack of scaffold diversity of these gaseous alkenes and alkynes may limit their broad usage in the synthesis of complex molecular scaffolds.

Employing gaseous alkanes as synthetic feedstock is attractive from an economic standpoint, but it is usually difficult to activate these gaseous alkanes due to their strong C(sp<sup>3</sup>)-H bonds. The harsh conditions required to activate such bonds would often lead to solvent functionalization or over-functionalization of products. Several recent reports on photo-mediated hydrogen atom transfer catalysis have led to promising results enabling functionalization of these inactive alkanes under mild conditions. The transformations can be potentially scaled up by taking advantage of the continuous-flow reactors. However, the efficient functionalization of methane, which is the most appealing but challenging substrate, is still difficult to achieve.

The synthesis of value-added fine chemicals using gaseous reagents under photo conditions has been considered difficult-to-handle in the past. However, as shown in this review,



these reagents can now be safely and efficiently processed through photo-irradiated transformations to enable novel opportunities and applications in organic synthesis. The rapid development of photoredox and hydrogen atom transfer catalysis, together with the advanced micro-tubing reactors, offers great momentum to develop green and sustainable synthetic protocols for photosynthesis using gaseous reagents. The innovation will continue to grow, impact synthetic chemistry, and bring about great benefits for both pharmaceutical and chemical industries in the future.

### Acknowledgements

We thank Prof. Hou Jing (Nanjing University of Science and Technology) and Dr. Li Jiesheng (GSK-Singapore) for helpful discussion. We are grateful for the financial support provided by the National University of Singapore and GSK-EDB (R-143-000-687-592), the National University of Singapore Flagship Green Energy Program (R-279-000-553-646, and R-279-000-553-731), NUS (Suzhou) Research Institute, and National Natural Science Foundation of China (Grant No. 21871205).

### Conflict of interest

The authors declare no conflict of interest.

- [1] A. Tlili, X. Frogneux, E. Blondiaux, T. Cantat, *Angew. Chem. Int. Ed.* **2014**, *53*, 2543–2545; *Angew. Chem.* **2014**, *126*, 2577–2579.
- [2] a) L. Kollár, *Modern Carbonylation Methods*, Wiley-VCH, Weinheim, **2008**; b) M. Aresta, *Carbon Dioxide as Chemical Feedstock*, Wiley-VCH, Weinheim, **2010**; c) I.-T. Trotsuş, T. Zimmermann, F. Schüth, *Chem. Rev.* **2014**, *114*, 1761–1782; d) N. J. Gunsalus, A. Koppaka, S. H. Park, S. M. Bischof, B. G. Hashiguchi, R. A. Periana, *Chem. Rev.* **2017**, *117*, 8521–8573.
- [3] F. Fischer, *Brennst.-Chem.* **1930**, *11*, 489.
- [4] a) A. Haynes, P. M. Maitlis, G. E. Morris, G. J. Sunley, H. Adams, P. W. Badger, C. M. Bowers, D. B. Cook, P. I. P. Elliott, T. Ghaffar, H. Green, T. R. Griffin, M. Payne, J. M. Pearson, M. J. Taylor, P. W. Vickers, R. J. Watt, *J. Am. Chem. Soc.* **2004**, *126*, 2847–2861; b) T. W. Dekleva, D. Forster, *J. Am. Chem. Soc.* **1985**, *107*, 3565–3567.
- [5] a) K. Nagahara, I. Ryu, N. Kambe, M. Komatsu, N. Sonoda, *J. Org. Chem.* **1995**, *60*, 7384–7385; b) W. T. Boese, A. S. Goldman, *Tetrahedron Lett.* **1992**, *33*, 2119–2122; c) A. Bakac, J. H. Espenson, V. G. Young, Jr., *Inorg. Chem.* **1992**, *31*, 4959–4964.
- [6] K. Faltings, *Ber. Dtsch. Chem. Ges. A* **1939**, *72*, 1207–1215.
- [7] I. Ryu, H. Muraoka, N. Kambe, M. Komatsu, N. Sonoda, *J. Org. Chem.* **1996**, *61*, 6396–6403.
- [8] P. J. Kropp, *Acc. Chem. Res.* **1984**, *17*, 131–137.
- [9] K. Nagahara, I. Ryu, M. Komatsu, N. Sonoda, *J. Am. Chem. Soc.* **1997**, *119*, 5465–5466.
- [10] I. Ryu, K. Nagahara, N. Kambe, N. Sonoda, S. Kreimerman, M. Komatsu, *Chem. Commun.* **1998**, 1953–1954.
- [11] a) O. Itsenko, T. Kihlberg, B. Långström, *J. Org. Chem.* **2004**, *69*, 4356–4360; b) O. Itsenko, B. Långström, *J. Org. Chem.* **2005**, *70*, 2244–2249; c) B. Långström, O. Itsenko, O. Rahman, *J. Labelled Compd. Radiopharm.* **2007**, *50*, 794–810; d) O. Itsenko, T. Kihlberg, B. Långström, *Eur. J. Org. Chem.* **2005**, 3830–3834.
- [12] T. Kawamoto, A. Sato, I. Ryu, *Chem. Eur. J.* **2015**, *21*, 14764–14767.
- [13] R. R. Ferguson, R. H. Crabtree, *J. Org. Chem.* **1991**, *56*, 5503–5510.
- [14] B. S. Jaynes, C. L. Hill, *J. Am. Chem. Soc.* **1995**, *117*, 4704–4705.
- [15] I. Ryu, A. Tani, T. Fukuyama, D. Ravelli, M. Fagnoni, A. Albin, *Angew. Chem. Int. Ed.* **2011**, *50*, 1869–1872; *Angew. Chem.* **2011**, *123*, 1909–1912.
- [16] a) K. Yamada, M. Okada, T. Fukuyama, D. Ravelli, M. Fagnoni, I. Ryu, *Org. Lett.* **2015**, *17*, 1292–1295; b) M. Okada, T. Fukuyama, K. Yamada, I. Ryu, D. Ravelli, M. Fagnoni, *Chem. Sci.* **2014**, *5*, 2893–2898.
- [17] I. Ryu, A. Tani, T. Fukuyama, D. Ravelli, S. Montanaro, M. Fagnoni, *Org. Lett.* **2013**, *15*, 2554–2557.
- [18] Q.-Q. Zhou, W. Guo, W. Ding, X. Wu, X. Chen, L.-Q. Lu, W.-J. Xiao, *Angew. Chem. Int. Ed.* **2015**, *54*, 11196–11199; *Angew. Chem.* **2015**, *127*, 11348–11351.
- [19] C. Gosset, S. Pellegrini, R. Jooris, T. Bousquet, L. Pelinski, *Adv. Synth. Catal.* **2018**, *360*, 3401–3405.
- [20] N. Micic, A. Polyzos, *Org. Lett.* **2018**, *20*, 4663–4666.
- [21] B. Lu, Y. Cheng, L.-Y. Chen, J.-R. Chen, W.-J. Xiao, *ACS Catal.* **2019**, *9*, 8159–8164.
- [22] N. A. Romero, D. A. Nicewicz, *Chem. Rev.* **2016**, *116*, 10075–10166.
- [23] W. Guo, L.-Q. Lu, Y. Wang, Y.-N. Wang, J.-R. Chen, W.-J. Xiao, *Angew. Chem. Int. Ed.* **2015**, *54*, 2265–2269; *Angew. Chem.* **2015**, *127*, 2293–2297.
- [24] M. Majek, A. Jacobi von Wangelin, *Angew. Chem. Int. Ed.* **2015**, *54*, 2270–2274; *Angew. Chem.* **2015**, *127*, 2298–2302.
- [25] a) L.-J. Gu, C. Jin, J.-Y. Liu, *Green Chem.* **2015**, *17*, 3733–3736; b) H.-T. Zhang, L.-J. Gu, X.-Z. Huang, R. Wang, C. Jin, G.-P. Li, *Chin. Chem. Lett.* **2016**, *27*, 256–260.
- [26] a) A. Cartier, E. Levernier, V. Corcé, T. Fukuyama, A. L. Dhimane, C. Ollivier, I. Ryu, L. Fensterbank, *Angew. Chem. Int. Ed.* **2019**, *58*, 1789–1793; *Angew. Chem.* **2019**, *131*, 1803–1807; b) V. Corcé, L.-M. Chamoreau, E. Derat, J.-P. Goddard, C. Ollivier, L. Fensterbank, *Angew. Chem. Int. Ed.* **2015**, *54*, 11414–11418; *Angew. Chem.* **2015**, *127*, 11576–11580.
- [27] A. Cartier, E. Levernier, A.-L. Dhimane, T. Fukuyama, C. Ollivier, I. Ryu, L. Fensterbank, *Adv. Synth. Catal.* **2020**, *362*, 2254–2259.
- [28] a) T. Kondo, Y. Tsuji, Y. Watanabe, *Tetrahedron Lett.* **1988**, *29*, 3833–3836; b) T. Ishiyama, N. Miyaoura, A. Suzuki, *Tetrahedron Lett.* **1991**, *32*, 6923–6926.
- [29] S. Sumino, A. Fusano, T. Fukuyama, I. Ryu, *Acc. Chem. Res.* **2014**, *47*, 1563–1574.
- [30] A. Fusano, S. Sumino, S. Nishitani, T. Inouye, K. Morimoto, T. Fukuyama, I. Ryu, *Chem. Eur. J.* **2012**, *18*, 9415–9422.
- [31] a) A. Fusano, T. Fukuyama, S. Nishitani, T. Inouye, I. Ryu, *Org. Lett.* **2010**, *12*, 2410–2413; b) S. Sumino, T. Ui, I. Ryu, *Org. Lett.* **2013**, *15*, 3142–3145; c) A. Fusano, S. Sumino, T. Fukuyama, I. Ryu, *Org. Lett.* **2011**, *13*, 2114–2117; d) S. Roslin, L. R. Odell, *Chem. Commun.* **2017**, *53*, 6895–6898; e) I. Ryu, S. Kreimerman, F. Araki, S. Nishitani, Y. Oderaotoshi, S. Minakata, M. Komatsu, *J. Am. Chem. Soc.* **2002**, *124*, 3812–3813; f) T. Fukuyama, T. Inouye, I. Ryu, *J. Organomet. Chem.* **2007**, *692*, 685–690.
- [32] T. Fukuyama, S. Nishitani, T. Inouye, K. Morimoto, I. Ryu, *Org. Lett.* **2006**, *8*, 1383–1386.
- [33] G. M. Torres, Y. Liu, B. A. Arndtsen, *Science* **2020**, *368*, 318–323.
- [34] a) A. A. Olajire, *J. CO<sub>2</sub> Util.* **2013**, *3–4*, 74–92; b) A. Tortajada, F. Juliá-Hernández, M. Börjesson, T. Moragas, R. Martín, *Angew. Chem. Int. Ed.* **2018**, *57*, 15948–15982; *Angew. Chem.* **2018**, *130*, 16178–16214; c) J. Hou, J.-S. Li, J. Wu, *Asian J. Org. Chem.* **2018**, *7*, 1439–1447; d) C. S. Yeung, *Angew. Chem. Int. Ed.* **2019**, *58*, 5492–5502; *Angew. Chem.* **2019**, *131*, 5546–5556.



- [35] a) S. Tazuke, H. Ozawa, *J. Chem. Soc. Chem. Commun.* **1975**, 237–238; b) S. Tazuke, S. Kazama, N. Kitamura, *J. Org. Chem.* **1986**, 51, 4548–4553; c) Y. Ito, Y. Uozu, T. Matsuura, *J. Chem. Soc. Chem. Commun.* **1988**, 562–564; d) T. Ogata, K. Hiranaga, S. Matsuoka, Y. Wada, S. Yanagida, *Chem. Lett.* **1993**, 22, 983–984.
- [36] a) I. I. F. Boogaerts, S. P. Nolan, *J. Am. Chem. Soc.* **2010**, 132, 8858–8859; b) L. Zhang, J.-H. Cheng, T. Ohishi, Z.-M. Hou, *Angew. Chem. Int. Ed.* **2010**, 49, 8670–8673; *Angew. Chem.* **2010**, 122, 8852–8855; c) K. Sasano, J. Takaya, N. Iwasawa, *J. Am. Chem. Soc.* **2013**, 135, 10954–10957; d) Z. Zhang, L.-L. Liao, S.-S. Yan, L. Wang, Y.-Q. He, J.-H. Ye, J. Li, Y.-G. Zhi, D.-G. Yu, *Angew. Chem. Int. Ed.* **2016**, 55, 7068–7072; *Angew. Chem.* **2016**, 128, 7184–7188; e) I. I. F. Boogaerts, G. C. Fortman, M. R. L. Furst, C. S. J. Cazin, S. P. Nolan, *Angew. Chem. Int. Ed.* **2010**, 49, 8674–8677; *Angew. Chem.* **2010**, 122, 8856–8859.
- [37] Y. Masuda, N. Ishida, M. Murakami, *J. Am. Chem. Soc.* **2015**, 137, 14063–14066.
- [38] N. Ishida, Y. Masuda, S. Uemoto, M. Murakami, *Chem. Eur. J.* **2016**, 22, 6524–6527.
- [39] H. Seo, M. H. Katcher, T. F. Jamison, *Nat. Chem.* **2017**, 9, 453–456.
- [40] N. Ishida, Y. Masuda, Y. Imamura, K. Yamazaki, M. Murakami, *J. Am. Chem. Soc.* **2019**, 141, 19611–19615.
- [41] H. Seo, A. Liu, T. F. Jamison, *J. Am. Chem. Soc.* **2017**, 139, 13969–13972.
- [42] K. Osakada, R. Sato, T. Yamamoto, *Organometallics* **1994**, 13, 4645–4647.
- [43] A. Correa, R. Martín, *J. Am. Chem. Soc.* **2009**, 131, 15974–15975.
- [44] M. Börjesson, T. Moragas, D. Gallego, R. Martín, *ACS Catal.* **2016**, 6, 6739–6749.
- [45] K. Shimomaki, K. Murata, R. Martin, N. Iwasawa, *J. Am. Chem. Soc.* **2017**, 139, 9467–9470.
- [46] Q.-Y. Meng, S. Wang, B. König, *Angew. Chem. Int. Ed.* **2017**, 56, 13426–13430; *Angew. Chem.* **2017**, 129, 13611–13615.
- [47] a) K. Shimomaki, T. Nakajima, J. Caner, N. Toriumi, N. Iwasawa, *Org. Lett.* **2019**, 21, 4486–4489; b) S. K. Bhunia, P. Das, S. Nandi, R. Jana, *Org. Lett.* **2019**, 21, 4632–4637.
- [48] C. Zhu, Y.-F. Zhang, Z.-Y. Liu, L. Zhou, H.-D. Liu, C. Feng, *Chem. Sci.* **2019**, 10, 6721–6726.
- [49] W.-J. Zhou, Z.-H. Wang, L.-L. Liao, Y.-X. Jiang, K.-G. Cao, T. Ju, Y.-W. Li, G.-M. Cao, D.-G. Yu, *Nat. Commun.* **2020**, 11, 3263.
- [50] L.-L. Liao, G.-M. Cao, J.-H. Ye, G.-Q. Sun, W.-J. Zhou, Y.-Y. Gui, S.-S. Yan, G. Shen, D.-G. Yu, *J. Am. Chem. Soc.* **2018**, 140, 17338–17342.
- [51] a) H. Hoberg, Y. Peres, C. Krüger, Y.-H. Tsay, *Angew. Chem. Int. Ed. Engl.* **1987**, 26, 771–773; *Angew. Chem.* **1987**, 99, 799–800; b) H. Hoberg, S. Gross, A. Milchereit, *Angew. Chem. Int. Ed. Engl.* **1987**, 26, 571–572; *Angew. Chem.* **1987**, 99, 567–569.
- [52] C. M. Williams, J. B. Johnson, T. Rovis, *J. Am. Chem. Soc.* **2008**, 130, 14936–14937.
- [53] a) M. D. Greenhalgh, S. P. Thomas, *J. Am. Chem. Soc.* **2012**, 134, 11900–11903; b) T. G. Ostapowicz, M. Schmitz, M. Krystof, J. Klankermayer, W. Leitner, *Angew. Chem. Int. Ed.* **2013**, 52, 12119–12123; *Angew. Chem.* **2013**, 125, 12341–12345; c) L. Wu, Q. Liu, I. Fleischer, R. Jackstell, M. Beller, *Nat. Commun.* **2014**, 5, 3091.
- [54] K. Murata, N. Numasawa, K. Shimomaki, J. Takaya, N. Iwasawa, *Chem. Commun.* **2017**, 53, 3098–3101.
- [55] Q.-Y. Meng, S. Wang, G. S. Huff, B. König, *J. Am. Chem. Soc.* **2018**, 140, 3198–3201.
- [56] V. R. Yatham, Y. Shen, R. Martin, *Angew. Chem. Int. Ed.* **2017**, 56, 10915–10919; *Angew. Chem.* **2017**, 129, 11055–11059.
- [57] M.-Y. Wang, Y. Cao, X. Liu, N. Wang, L.-N. He, S.-H. Li, *Green Chem.* **2017**, 19, 1240–1244.
- [58] Z.-B. Yin, J.-H. Ye, W.-J. Zhou, Y.-H. Zhang, L. Ding, Y.-Y. Gui, S.-S. Yan, J. Li, D.-G. Yu, *Org. Lett.* **2018**, 20, 190–193.
- [59] S. Sung, C. Zhou, J.-T. Yu, J. Cheng, *Org. Lett.* **2019**, 21, 6579–6583.
- [60] J.-H. Ye, M. Miao, H. Huang, S.-S. Yan, Z.-B. Yin, W.-J. Zhou, D.-G. Yu, *Angew. Chem. Int. Ed.* **2017**, 56, 15416–15420; *Angew. Chem.* **2017**, 129, 15618–15622.
- [61] J. Hou, A. Ee, H. Cao, H.-W. Ong, J.-H. Xu, J. Wu, *Angew. Chem. Int. Ed.* **2018**, 57, 17220–17224; *Angew. Chem.* **2018**, 130, 17466–17470.
- [62] H. Wang, Y. Gao, C. Zhou, G. Li, *J. Am. Chem. Soc.* **2020**, 142, 8122–8129.
- [63] Q. Fu, Z.-Y. Bo, J.-H. Ye, T. Ju, H. Huang, L.-L. Liao, D.-G. Yu, *Nat. Commun.* **2019**, 10, 3592.
- [64] B. Zhang, Y.-P. Yi, Z.-Q. Wu, C. Chen, C.-J. Xi, *Green Chem.* **2020**, 22, 5961–5965.
- [65] M. Schmalzbauer, T. D. Svejstrup, F. Fricke, P. Brandt, M. J. Johansson, G. Bergonzini, B. König, *Chem.* **2020**, <https://doi.org/10.1016/j.chempr.2020.08.022>.
- [66] L. Guo, F. Song, S. Zhu, H. Li, L. Chu, *Nat. Commun.* **2018**, 9, 4543.
- [67] a) K. Nogi, T. Fujihara, J. Terao, Y. Tsuji, *J. Am. Chem. Soc.* **2016**, 138, 5547–5550; b) X. Wang, M. Nakajima, R. Martin, *J. Am. Chem. Soc.* **2015**, 137, 8924–8927; c) T. Fujihara, Y. Tani, K. Semba, J. Terao, Y. Tsuji, *Angew. Chem. Int. Ed.* **2012**, 51, 11487–11490; *Angew. Chem.* **2012**, 124, 11655–11658; d) L. Zhang, J.-H. Cheng, B. Carry, Z.-M. Hou, *J. Am. Chem. Soc.* **2012**, 134, 14314–14317; e) T. Fujihara, T. Xu, K. Semba, J. Terao, Y. Tsuji, *Angew. Chem. Int. Ed.* **2011**, 50, 523–527; *Angew. Chem.* **2011**, 123, 543–547; f) S. Li, W. Yuan, S. Ma, *Angew. Chem. Int. Ed.* **2011**, 50, 2578–2582; *Angew. Chem.* **2011**, 123, 2626–2630.
- [68] J. Hou, A. Ee, W. Feng, J.-H. Xu, Y. Zhao, J. Wu, *J. Am. Chem. Soc.* **2018**, 140, 5257–5263.
- [69] T. Ju, Q. Fu, J.-H. Ye, Z. Zhang, L.-L. Liao, S.-S. Yan, X.-Y. Tian, S.-P. Luo, J. Li, D.-G. Yu, *Angew. Chem. Int. Ed.* **2018**, 57, 13897–13901; *Angew. Chem.* **2018**, 130, 14093–14097.
- [70] X. Fan, X. Gong, M. Ma, R. Wang, P. J. Walsh, *Nat. Commun.* **2018**, 9, 4936.
- [71] S. Wang, B.-Y. Cheng, M. Sršen, B. König, *J. Am. Chem. Soc.* **2020**, 142, 7524–7531.
- [72] a) S. Kikuchi, K. Sekine, T. Ishida, T. Yamada, *Angew. Chem. Int. Ed.* **2012**, 51, 6989–6992; *Angew. Chem.* **2012**, 124, 7095–7098; b) K. Sekine, A. Takayanagi, S. Kikuchi, T. Yamada, *Chem. Commun.* **2013**, 49, 11320–11322; c) W.-Z. Zhang, M.-W. Yang, X.-B. Lu, *Green Chem.* **2016**, 18, 4181–4184; d) C.-X. Guo, W.-Z. Zhang, H. Zhou, N. Zhang, X.-B. Lu, *Chem. Eur. J.* **2016**, 22, 17156–17159.
- [73] B. Sahoo, P. Bellotti, F. Juliá-Hernández, Q.-Y. Meng, S. Crespi, B. König, R. Martin, *Chem. Eur. J.* **2019**, 25, 9001–9005.
- [74] Q.-Y. Meng, T. E. Schirmer, A. L. Berger, K. Donabauer, B. König, *J. Am. Chem. Soc.* **2019**, 141, 11393–11397.
- [75] a) D. F. McMillen, D. M. Golden, *Annu. Rev. Phys. Chem.* **1982**, 33, 493–532; b) J. D. Cuthbertson, D. W. C. MacMillan, *Nature* **2015**, 519, 74–77; c) R. Zhou, Y. Y. Goh, H. Liu, H. Tao, L. Li, J. Wu, *Angew. Chem. Int. Ed.* **2017**, 56, 16621–16625; *Angew. Chem.* **2017**, 129, 16848–16852.
- [76] a) D. D. M. Wayner, D. J. McPhee, D. Griller, *J. Am. Chem. Soc.* **1988**, 110, 132–137; b) B. A. Sim, D. Griller, D. D. M. Wayner, *J. Am. Chem. Soc.* **1989**, 111, 754–755.
- [77] a) R. Alibés, P. de March, M. Figueredo, J. Font, M. Racamonde, *Tetrahedron Lett.* **2001**, 42, 6695–6697; b) H. Kosugi, S. Sekiguchi, R.-i. Sekita, H. Uda, *Bull. Chem. Soc. Jpn.* **1976**, 49, 520–528; c) B. Heller, B. Sundermann, H. Buschmann, H.-J. Drexler, J. You, U. Holzgrabe, E. Heller, G. Oehme, *J. Org. Chem.* **2002**, 67, 4414–4422; d) R. Alibés, P. de March, M. Figueredo, J. Font,



- X. Fu, M. Racamonde, Á. Álvarez-Larena, J. F. Piniella, *J. Org. Chem.* **2003**, 68, 1283–1289.
- [78] F. Xue, H. Deng, C. Xue, D. K. B. Mohamed, K. Y. Tang, J. Wu, *Chem. Sci.* **2017**, 8, 3623–3627.
- [79] J. Li, Y. Luo, H. W. Cheo, Y. Lan, J. Wu, *Chem* **2019**, 5, 192–203.
- [80] R. H. Crabtree, *Chem. Rev.* **1995**, 95, 987–1007.
- [81] a) R. A. Periana, O. Mironov, D. Taube, G. Bhalla, C. J. Jones, *Science* **2003**, 301, 814–818; b) V. N. Cavaliere, B. F. Wicker, D. J. Mindiola, in *Adv. Organomet. Chem.*, Vol. 60 (Eds.: A. F. Hill, M. J. Fink), **2012**, pp. 1–47; c) A. K. Cook, S. D. Schimler, A. J. Matzger, M. S. Sanford, *Science* **2016**, 351, 1421–1424; d) K. T. Smith, S. Berritt, M. González-Moreiras, S. Ahn, M. R. Smith III, M.-H. Baik, D. J. Mindiola, *Science* **2016**, 351, 1424–1427.
- [82] a) X. Wu, Y. Zhao, H. Ge, *J. Am. Chem. Soc.* **2014**, 136, 1789–1792; b) Y. Aihara, N. Chatani, *J. Am. Chem. Soc.* **2014**, 136, 898–901.
- [83] A. Hu, J.-J. Guo, H. Pan, Z. Zuo, *Science* **2018**, 361, 668–672.
- [84] H.-P. Deng, Q. Zhou, J. Wu, *Angew. Chem. Int. Ed.* **2018**, 57, 12661–12665; *Angew. Chem.* **2018**, 130, 12843–12847.
- [85] G. Laudadio, Y. Deng, K. van der Wal, D. Ravelli, M. Nuño, M. Fagnoni, D. Guthrie, Y. Sun, T. Noël, *Science* **2020**, 369, 92–96.

Manuscript received: August 5, 2020

Accepted manuscript online: October 1, 2020

Version of record online: ■ ■ ■ ■ ■ ■ ■ ■ ■ ■



## Reviews

## Photochemistry

B. Cai, H. W. Cheo, T. Liu,  
J. Wu\* ————— ■■■—■■■

Light-Promoted Organic Transformations  
Utilizing Carbon-Based Gas Molecules as  
Feedstocks

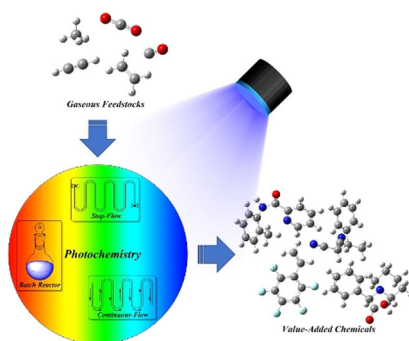


Photo-mediated fixation of carbon-based gas molecules: C–C bond formation utilizing carbon-based small gas molecules, including CO, CO<sub>2</sub>, acetylene, ethylene, ethane and methane, as feedstocks is attractive but challenging. The emergence of photoredox chemistry and the development of engineered flow technology have provided vast opportunities for gas conversions, which has gained tremendous momentum over the past decade.